



1

2 **Seasonal cycles and trends of water budget components in 18**
3 **river basins across Tibetan Plateau: a multiple datasets**
4 **perspective**

5

6 Wenbin Liu^a, Fubao Sun^{a*}, Yanzhong Li^a, Guoqing Zhang^{b,c},

7 Yan-Fang Sang^a, Jiahong Liu^d, Hong Wang^a, Peng Bai^a

8

9 ^aKey Laboratory of Water Cycle and Related Land Surface Processes, Institute of Geographic
10 Sciences and Natural Resources Research, Chinese Academy of Sciences, Beijing 100101, China

11 ^bKey Laboratory of Tibetan Environmental Changes and Land Surface Processes, Institute of
12 Tibetan Plateau Research, Chinese Academy of Sciences, Beijing 100101, China

13 ^cCAS Center for Excellent in Tibetan Plateau Earth Sciences, Beijing 100101, China

14 ^dKey Laboratory of Simulation and Regulation of Water Cycle in River Basin, China Institute of
15 Water Resources and Hydropower Research, Beijing 100038, China

16

17 **Submitted to:** Hydrology and Earth System Sciences

18 **Corresponding Author:** Dr. Fubao Sun (Sunfb@igsnr.ac.cn), from the Key Laboratory of Water
19 Cycle and Related Land Surface Processes, Institute of Geographic Sciences and Natural
20 Resources Research, Chinese Academy of Sciences (No. A11, Datun Road, Chaoyang District,
21 Beijing 100101, China)

22 **Email Addresses for other authors:** Wenbin Liu (liuwb@igsnr.ac.cn), Yanzhong Li
23 (liy.z.14b@igsnr.ac.cn), Guoqing Zhang (guoqing.zhang@itpcas.ac.cn), Yan-fang Sang
24 (sangyf@igsnr.ac.cn), Jiahong Liu (liujh@iwhr.com), Hong Wang (wanghong@igsnr.ac.cn),
25 Peng Bai (baip.11b@igsnr.ac.cn)

26

27

2016/11/25

28



29 **Highlights**

- 30 ● Monthly basin-wide ET was calculated through water balance considering the
31 impacts of glacier and water storage change
- 32 ● Water budget components and trends for 18 river basins over TP were evaluated
- 33 ● Uncertainties were discussed from multiple dataset perspective

34



35 **Abstract.** The insights of water budgets over Tibetan Plateau (TP) are not fully
36 understood so far due to the lack of quantitative observations of the land surface
37 processes. Here, we investigated the seasonal cycles and trends of water budget
38 components in 18 TP basins through the use of multi-source datasets during the period
39 1982-2011. A two-step bias correction procedure was applied to calculate the
40 basin-wide evapotranspiration (ET) through the water balance considering the
41 influences of glacier and water storage change. The results indicated that precipitation,
42 which mainly concentrated during June-October (varied among different monsoons
43 impacted basins), is the major contributor to the runoff in TP basins. The basin-wide
44 snow water equivalent (SWE) was relatively higher from mid-autumn to spring for
45 most TP basins. The water cycles intensified under a global warming in most basins
46 except for the upper Yellow and Yalong Rivers, which were significantly influenced
47 by the weakening East Asian monsoon. Corresponded to the climate warming and
48 moistening in the TP and western China, the aridity index (PET/P) in most basins
49 decreased. The general hydrological regimes could be inferred from the perspective of
50 multi-source datasets although there are considerable uncertainties from different
51 datasets, which are comparable to some existing studies using the field observations
52 and complex modeling approaches. The results highlighted the usefulness of
53 integrating the multi-source data (e.g., in situ observations, remote sensing products,
54 reanalysis, land surface model simulations and climate model outputs) for
55 hydrological applications in the data-sparse environments and could be benefit for



56 understanding the water and energy budgets, sustainable management of water
57 resources under a warming climate in the harsh and data-sparse Tibetan Plateau.
58

59 **1 Introduction**

60 As the highest plateau in the globe (the average elevation is higher than 4000 meters
61 above the sea level), Tibetan Plateau (TP, also called “the roof of the world” or “the
62 third Pole”) is one of the most vulnerable region under a warming climate and is
63 subjected to strong interactions among atmosphere, hydrosphere, biosphere and
64 cryosphere in the earth system (Duan and Wu, 2006; Yao et al., 2012; Liu W. et al.,
65 2016b). It also serves as the “Asian water tower” with many major Asian rivers such
66 as Yellow river, Yangtze river, Brahmaputra river, Mekong river, Indus river, etc.,
67 originate from, which provides a vital water resource to support hundreds of millions
68 of people in China and the surrounding countries (Immerzell et al., 2010; Zhang et al.,
69 2013). Knowledge about the water budgets and their responses to the changing
70 environment is thus crucial for understanding the hydrological regimes and for
71 sustainable water resources management as well as environmental protection in this
72 special region (Yang et al., 2014; Chen et al., 2015).

73

74 TP is also known as a typical data-sparse mountain region which brings great
75 challenges to hydrological and related land surface studies (Zhang et al., 2007; Li F. et
76 al., 2013; Liu X. et al., 2016). For example, since the 1950s, totally 750 stations have
77 been established over China by the Chinese Meteorological Administration (CMA),
78 among which only less than 80 stations are distributed over the plateau (Wang and
79 Zeng, 2012). They are primary sparse and unevenly located at relatively low elevation
80 regions, focus only on the meteorological variables and lack of other land surface



81 observations such as evapotranspiration, snow water equivalent and latent heat fluxes,
82 etc.. In addition, long-term consecutive observations of river discharge, snow depth,
83 lake depth and glacier melts in TP are also absent (Akhta et al., 2009; Ma et al., 2016).
84 Therefore, the insights of water balance over various TP river basins locates at
85 different monsoon-dominant regions are, to some extent, still unclear so far due to the
86 lack of quantitative observations of the land surface processes (Cuo et al., 2014; Xu et
87 al., 2016). One way to break this limitation is to install more instruments to measure
88 the point scale water budgets (Yang et al., 2013; Zhou et al., 2013; Ma et al., 2015),
89 but it is extremely expensive to maintain long-term observations at the harsh
90 environment and is often difficult to be applied to basin or regional scales. Another
91 more popular way is to simulate basin-wide water budgets through physical-based
92 land surface models at several large river basins forced with remote sensing data and
93 large-scale gridded meteorological forcing datasets (Bookhagen and Burbank, 2010;
94 Xue et al., 2013; Zhang et al., 2013; Cuo et al., 2015; Zhou et al., 2015; Wang et al.,
95 2016). However, it is also limited by the lack of adequate data for model
96 calibration/validation and is hard to be used to multiple basins especially to relatively
97 smaller basins under the complex terrains (Li F. et al., 2014).

98
99 In recent years, a number of global (or regional) datasets for water budget components
100 have been released including remote sensing-based retrievals (Tapley et al., 2004;
101 Zhang et al., 2010; Long et al., 2014; Zhang Y. et al., 2016), land surface model (LSM)
102 simulations (Rui, 2011), reanalysis outputs (Berrisford et al., 2011; Kobayashi et al.,
103 2015) and gridded forcing data interpolated from the in situ observations (Harries et
104 al., 2014). For example, there are considerable products for terrestrial
105 evapotranspiration (ET) such as GLEAM_E (Global Land surface Evaporation: the



106 Amsterdam Methodology, Miralles et al., 2011a), MTE_E (a product integrated the
107 point-wise ET observation at FLUXNET sites with geospatial information extracted
108 from surface meteorological observations and remote sensing in a machine-learning
109 algorithm, Jung et al., 2010), LSM-simulated ETs from Global Land Data
110 Assimilation System version 2 (GLDAS-2) with different land surface schemes
111 (Rodell et al., 2004), ETs from Japanese 55-year reanalysis (JRA55_E), the
112 ERA-Interim global atmospheric reanalysis dataset (ERA-Interim) and the National
113 Aeronautic and Space Administration (NASA) Modern Era Retrospective-analysis
114 for Research and Application (MERRA) reanalysis data (Lucchesi, 2012). Moreover,
115 there are also several global or regional LSM-based runoff simulations from GLDAS
116 and the Variable Infiltration Capacity (VIC) model (Zhang et al., 2014). A few
117 attempts have been made to validate multiple datasets for certain water budget
118 component and to explore their possible hydrological implications, for example, Li X.
119 et al. (2014) and Liu W. et al. (2016a) evaluated multiple ET estimates against the
120 water balance method at annual and monthly time scales. Bai et al. (2016) assessed
121 streamflow simulations of GLDAS LSMs in five major rivers over TP based on the
122 discharge observations. Although there are certain uncertainties among different
123 datasets with various spatial and temporal resolutions and calculated through different
124 algorithms (Xia et al., 2012), they do provide a great chance for us to quantify the
125 general basin-wide water budgets and their uncertainties in gauge-sparse regions such
126 as TP considered in this study.

127

128 The objectives of this study are (1) to investigate the general water budgets in 18 river
129 basins across Tibetan Plateau from the perspective of multiple datasets, and (2) to
130 evaluate the seasonal cycles and annual trends of water budget components for 18 TP



131 basins. The paper is organized as follows: the datasets and methods applied in this
132 study are described in Sect.2. The results of season cycles and annual trends of water
133 budget components for 18 TP basins are presented and discussed in Sect.3. The
134 uncertainties inherited from multiple datasets are also discussed. In the Sect.4, we
135 summarized the general results which would helpful for understanding the water
136 balances of TP Rivers located at westerlies-dominated, Indian monsoon-dominated
137 and East Asian monsoon-dominated regions.

138

139 **2 Data and Method**

140 **2.1 Multiple datasets used**

141 **2.1.1 Study basins**

142 Eighteen river basins over TP (Fig.1) with the drainage area ranging from 2832 to
143 191235 km² (Table 1) are chosen in this study due to the availability of runoff data
144 during the period 1982-2011. They mainly locate at the northwestern, southeastern
145 and eastern parts of the plateau with multiyear-mean and basin-averaged temperature
146 and precipitation ranging from -5.68 to 0.97 °C and 128 to 717 mm, which are solely
147 or combined controlled by the westerlies, the Indian Summer monsoon and the Easter
148 Asian monsoon (Yao et al., 2012). The altitudes of the lowest and highest
149 hydrological gauging stations are 1650 m and 4982 m above the sea level. The glacier
150 and snow covers are relatively more for the westerlies-dominant basins such as
151 Yerqiang, Yulongkashi and Keliya (10.86~23.27% and 29.16~35.95%, respectively)
152 whereas are less for the East Asian monsoon-dominated basins such as Yellow,
153 Yangtze and Bayin (0~0.96% and 9.42~20.05%, respectively) (Table 1).

154 [<Figure 1, here please, thanks>](#)

155 [<Table 1, here please, thanks>](#)



156 **2.1.2 Runoff, Precipitation and Terrestrial storage change**

157 Observed daily runoff (Q) during the period 1982-2011 used for water balance
158 calculation for 18 TP basins was obtained from the National Hydrology Almanac of
159 China (Table 2). There are < 30% missing data in some gauging stations such as
160 Yajiang, Tongren, Gandatan and Zelingou. Therefore, the VIC Retrospective Land
161 Surface Dataset over China (1952~2012, VIC_IGSNRR simulated) with a spatial
162 resolution of 0.25 degree and a daily temporal resolution from the Geographic
163 Sciences and Natural Resources Research (IGSNRR), Chinese Academy of Sciences,
164 is also used, which is derived from the VIC model forced by the gridded daily
165 observed forcing (IGSNRR_forcing) (Zhang et al., 2014). A degree-day scheme was
166 used in the model to consider the influences of snow and glacier on hydrological
167 processes. In this study, we first assess the VIC_IGSNRR simulated runoff against the
168 observations for each basin (for example, at Tangnaihaid and Pangduo stations in
169 Fig.2). The VIC_IGSNRR simulated runoff is acceptable and could be used to replace
170 the missing values for a given basin, if the Nash Efficiency coefficient (NSE) between
171 the observation and simulation is above 0.65.

172 [< Figure 2, here please, thanks >](#)

173 Monthly gridded precipitation dataset (0.5 degree, 1961-2011) from CMA, which was
174 interpolated from observations of 2472 national meteorological stations using the
175 Thin Plate Spline method, was used in this study (Table 2). Considering the
176 uncertainty of CMA precipitation over TP due to the relatively sparse stations used
177 and the complex terrain conditions, two other precipitation datasets (IGSNRR_forcing
178 and TRMM (Tropical Rainfall Measuring Mission) 3B43 V7, Huffman et al., 2012)
179 were also applied. The precipitation from IGSNRR forcing datasets (0.25 degree) was
180 derived by interpolating gauged daily precipitation from 756 CMA stations based on



181 the synergraphic mapping system algorithm (Shepard, 1984; Zhang et al., 2014) and
182 was further bias-corrected using the CMA gridded precipitation. The CMA
183 precipitation is perfectly consistent with TRMM (Corr = 0.86, RMSE = 8.34
184 mm/month) and IGSNRR forcing (Corr = 0.94, RMSE = 7.15mm/month)
185 precipitation for multiple basins (and also for the smallest basin above Tongren station,
186 Fig.2), which reveals the applicability of CMA precipitation under the TP conditions.

187 [<Table 2, here please, thanks>](#)

188 Three latest global terrestrial water storage anomaly and water storage change (ΔS)
189 datasets (available on the GRACE Tellus website: <http://grace.jpl.nasa.gov/>) retrieved
190 from the Gravity Recovery and Climate Experiment (GRACE, Tapley et al., 2004;
191 Landerer and Swenson, 2012; Long et al., 2014), which were processed separately at
192 the Jet Propulsion Laboratory (JPL), the GeoForschungsZentrum (GFZ) and the
193 Center for Space Research at the University of Texas (CSR), were used. The GRACE
194 retrievals (2002-2013) from three processing centers were averaged and a glacier
195 isostatic adjustment correction as well a destriping filter were applied to minimize the
196 errors and uncertainties of extracted ΔS .

197

198 **2.1.3 Temperature, potential evaporation and ET**

199 The CMA monthly gridded temperature (0.5 degree) and potential evaporation (PET)
200 dataset (0.5 degree, Harris et al., 2013) from Climatic Research Unit (CRU) in the
201 University of East Anglia were used in this study. Moreover, six published
202 global/regional ET products (four diagnostic products and two LSMs simulations,
203 Table 2), namely (1) GLEAM_E (Miralles et al., 2010, 2011), which estimated three
204 sources of ET (transpiration, soil evaporation and interception) separately through



205 bare soil, short vegetation and vegetation with a tall canopy through a set of algorithm
206 (www.gleam.eu), (2) GNoah_E simulated by GLDAS-2 with the Catchment Noah
207 scheme (<http://disc.sci.gsfc.nasa.gov/hydrology/data-holdings>) (Rodell et al., 2004),
208 (3) Zhang_E (Zhang et al., 2010) estimated using the modified Penman-Monteith
209 approach forced with MODIS data, satellite-based vegetation parameters and
210 meteorological observations (<http://www.nts.gov.au/project/et>), (4) MET_E (Jung
211 et al., 2010) (<https://www.bgc-jena.mpg.de/geodb/projects/Home.phs>), (5) VIC_E
212 (Zhang et al., 2014) from VIC_IGSNRR simulations
213 (http://hydro.igsnrr.ac.cn/public/vic_outputs.html) and (6) PML_E (Zhang Y. et al.,
214 2016) computed from global observation-driven Penman-Monteith-Leuning (PML)
215 model (<https://data.csiro.au/dap/landingpage?pid=csiro:17375&v=2&d=true>).

216

217 **2.1.4 Vegetation and snow/glacier parameters**

218 Two vegetation parameter datasets, the Normalized Difference Vegetation Index
219 (NDVI) and the Leaf Area Index (LAI) were used to quantify the dynamics of
220 vegetation for 18 TP basins (Table 2). The NDVI data was obtained from the Global
221 Inventory Modeling and Mapping Studies (GIMMS) (Turker et al., 2005)
222 (https://nex.nasa.gov/nex/projects/1349/wiki/general_data_description_and_access/)
223 while the LAI data was collected from the Global Land Surface Satellite (GLASS)
224 products (<http://www.glcfc.umd.edu/data/lai/>) (Liang and Xiao, 2012). Seasonal snow
225 and glacier are widespread over the plateau which significantly influences the water
226 and energy budgets in TP, but their observations are difficult due to the harsh
227 environment, especially at the basin scale. However, there are currently a few
228 satellite-based or LSM-simulated products which could provide general information



229 about the variations of snow and glacier. The daily cloud free snow composite product
230 from MODIS Terra-Aqua and the Interactive Multisensor Snow and Ice Mapping
231 System for the Tibetan Plateau was applied to quantify the snow cover changes for
232 each basin (Zhang et al., 2012; Yu et al., 2015). The snow water equivalent (SWE)
233 retrieved from Global Snow Monitoring for Climate Research product (GlobSnow-2,
234 <http://www.globsnow.info/>) and the VIC_IGSNRR simulations were also used in this
235 study (Takala et al., 2011; Zhang et al., 2014). Moreover, the Second Glacier
236 Inventory Dataset of China was used to extract the general distribution of glacier
237 (Guo et al., 2014). All gridded datasets used were first uniformly interpolated to a
238 spatial resolution of 0.5 degree to make their inter-comparison possible. The datasets
239 were then extracted for each of TP basins.

240

241 **2.1.5 Monsoon indices**

242 The TP climate is generally influenced by the westerlies, Indian summer monsoon and
243 East Asian summer monsoon (Yao et al., 2012). To investigate the changes of
244 monsoon systems and their potential influences on the water budget in TP basins,
245 three monsoon indices, namely Asian Zonal Circulation Index (AZCI), Indian Ocean
246 Dipole Mode Index (IODMI) and East Asian Summer Monsoon Index (EASMI), are
247 also used in this study. The IODMI is an indicator of the east-west temperature
248 gradient across the tropical Indian Ocean defined by Saji et al. (1999), which can be
249 downloaded from the following website:

250 [http://www.jamstec.go.jp/frcgc/research/d1/iod/HTML/Dipole%20Mode%20Index.ht](http://www.jamstec.go.jp/frcgc/research/d1/iod/HTML/Dipole%20Mode%20Index.html)
251 [ml](http://www.jamstec.go.jp/frcgc/research/d1/iod/HTML/Dipole%20Mode%20Index.html). The EASMI and AZCI (60°-150°E) reflect the dynamics of East Asian summer

252 monsoon (Li and Zeng, 2002) and the westerlies, which can be obtained from the

253 <http://ljp.gcess.cn/dct/page/65577> and the National Climate Center of China



254 (<http://ncc.cma.gov.cn/Website/index.php?ChannelID=43WCHID=5>), respectively.

255 **2.2 Methods**

256 **2.2.1 Water balance-based ET estimation**

257 The basin-wide water balance at the monthly and annual timescales could
258 traditionally be written as the principle of mass conservation (also known as the
259 continuity equation, Oliverira et al., 2014) of basin-wide precipitation (P, mm),
260 evapotranspiration (ET_{wb} , mm), runoff (Q, mm) as well as terrestrial water storage
261 change (ΔS , mm),

$$262 \quad ET_{wb} = P - Q - \Delta S \quad (1)$$

263 In most TP basins, glacier melt (M_G) contributes to river discharge together with
264 precipitation (liquid precipitation and snow). The monthly and annual water balance
265 in these basins can thus be revised as,

$$266 \quad ET_{wb} = P + M_G - Q - \Delta S \quad (2)$$

267 Several attempts have been made for separating glacier contributions to river
268 discharge through site-scale isotopic observations, remote sensing as well as
269 land-surface hydrological modeling for some individual TP basins (Zhang et al., 2013;
270 Zhou et al., 2014; Neckel et al., 2014). However, accurate quantification of M_G is
271 difficult in data-sparse TP, especially for multiple basins. In this study, we simply use
272 the percentages of glacier melt to river discharge for some TP basins concluded from
273 the existing studies (Chen, 1988; Mansur and Ajnis, 2005; Zhang et al., 2013; Liu J. et
274 al., 2016) and the empirical relations between the glacier area ratio (%) and glacier
275 melt in basins mentioned above (Table 3).

276 [<Table 3, here please, thanks>](#)

277 The terrestrial water storage (ΔS) in Eq.(2), which includes the surface, subsurface
278 and ground water changes, cannot be neglected in water balance calculation at a



279 monthly or annual timescale due to snow accumulation and some anthropogenic
280 interferences such as reservoir regulation and agriculture irrigation (Liu W. et al.,
281 2016a). The water balance-based ET (ET_{wb}) during 2002-2011 can be calculated
282 through Eq. (2) using the GRACE-derived mass anomaly as ΔS . For ET_{wb}
283 calculation before 2002 when the GRACE data is unavailable, we use a two-step bias
284 correction procedure (Li X. et al., 2014) to close the water balance for 18 basins at
285 monthly timescale considering the ΔS . We define $P + M_G - Q$ as biased ET
286 (ET_{biased} , available from 1982-2011) relative to the ET_{wb} (available from 2002-2011
287 when the GRACE data is available) calculated from Eq. (2). Firstly, the ET_{biased} and
288 ET_{wb} series over the period 2002-2011 were separately fitted using a gamma
289 distribution, which has been evidenced as an proper method for modeling the
290 probability distribution of ET (Bouraoui et al., 1999). The value in monthly ET_{biased}
291 series (2002-2011) can be bias-corrected through the inverse function (F^{-1}) of the
292 gamma cumulative distribution function (CDF, F) of ET_{wb} by matching the
293 cumulative probabilities between two CDFs as follow (Liu W. et al., 2016a),

$$294 \quad ET_{wb}(m) = F^{-1}(F(ET_{biased}(m)|\alpha_{biased}, \beta_{biased})|\alpha_{wb}, \beta_{wb}) \quad (3)$$

295 Here α_{biased} , β_{biased} , α_{wb} and β_{wb} are the shape and scale parameters of gamma
296 distribution for ET_{biased} and ET_{wb} . The second step is to eliminate the annual bias
297 through the ratio of annual ET_{biased} to annual ET_{wb} calculated in the first step using
298 the following method,

$$299 \quad ET_{wb}(m) = \frac{ET_{biased}(a)}{ET_{wb}(a)} \times ET_{wb}(m) \quad (4)$$

300 The procedure was then applied to correct the monthly ET_{biased} series and calculated
301 the monthly ET_{wb} during the period 1982-2001 for all TP basins. The ET_{wb} obtained
302 was seemed as the “true” ET for evaluating multiple ET products and further for the
303 trend analysis.



304 **2.2.2 Modified Mann-Kendall test method**

305 The Mann-Kendall (MK) test is a rank-based nonparametric approach and is less
306 sensitive to outlier relative to other parametric statistics. However, it is sometimes
307 impacted by the serial correlation of time series. In this study, we use a modified
308 version of MK test (MMK, Hamed and Rao, 1998) to quantify the trends of water
309 budget components in 18 TP basins. The MMK considers the lag- i autocorrelation and
310 related robustness of the autocorrelation, which has been widely used in previous
311 studies during the last five decades (McVicar et al., 2012; Liu and Sun, 2016).

312

313 **3 Results and Discussion**

314 **3.1 ET evaluation and General hydrological characteristics of 18 TP basins**

315 We first evaluated monthly performances of six ET products in 18 TP basins against
316 the ET_{wb} , which was calculated through water balance considering the impacts of
317 glacier and water storage change (Fig. 3). The ranges of monthly averaged ET among
318 different basins (approximately 4–39 mm month⁻¹) are very close for all products
319 compare with that calculated from the ET_{wb} (6–42 mm month⁻¹). However,
320 GLEAM_E (correlation coefficient: Corr = 0.85 and root-mean-square-error: RMSE =
321 5.69 mm month⁻¹) and VIC_E (Corr = 0.82 and RMSE = 6.16 mm month⁻¹) perform
322 relatively better than others. Although Zhang_E and GNoah_E were found closely
323 correlated to monthly ET_{wb} in the upper Yellow River, the upper Yangtze River,
324 Qiangtang and Qaidam basins (Li X. et al., 2014), they did not exhibit overall good
325 performances (Corr = 0.61, RMSE = 7.97 mm month⁻¹ for Zhang_E and Corr = 0.42,
326 RMSE = 10.16 mm month⁻¹ for GNoah_E) for 18 TP basin used in this study. We thus
327 use GLEAM_E and VIC_E together with ET_{wb} to calculate the seasonal cycles and
328 trends of ET in 18 TP basins in the following sections.



329 [< Figure 3, here please, thanks >](#)

330 To investigate the general hydroclimatic characteristics of rivers over TP, we classify

331 18 basins into three categories, namely westerlies-dominated basins (Yerqiang,

332 Yulongkashi and Kelia), Indian monsoon-dominated basins (Brahmaputra and

333 Salween), and East Asian monsoon-dominated basins (Yellow, Yalong and Yangtze)

334 referred to Tian et al. (2007) and Yao et al. (2012, 2013). Interestingly, they are

335 clustered into three groups under the perspective of Budyko framework (Budyko,

336 1974; Zhang D. et al., 2016) with relatively lower evaporative index for Indian

337 monsoon-dominant basins and higher aridity index for westerlies-dominant basins,

338 which reveal various long-term hydroclimatologic conditions (Fig. 4). Overall, the

339 annual mean air temperature increases (-5.68~0.97 °C) while multiyear mean glacier

340 area (and thus the glacier melt normalized by precipitation) decreases (23.27 ~ 0%)

341 gradually from the westerlies-dominant, Indian monsoon-dominant to East Asian

342 monsoon-dominant basins. The vegetation status (NDVI range: 0.05~0.43; LAI range:

343 0.03~0.83) tends to be better and ET increases (and thus runoff coefficient gradually

344 decreases) from cold to warm basins (Fig. 4 and Table 1). It is a general picture of

345 hydrological regime in high-altitude and cold regions (Zhang et al., 2013; Cuo et al.,

346 2014), which could be interpreted from the perspective of multi-source datasets in

347 data-sparse TP.

348 [< Figure 4, here please, thanks >](#)

349 **3.2 Seasonal cycles of basin-wide water budget components for TP basins**

350 The multi-year means of water budget components (i.e., P, Q, ET, snow cover and

351 SWE) and vegetation parameters (i.e., NDVI and LAI) were calculated for each

352 calendar month and for 18 TP river basins over using multi-source datasets available

353 from 1982 to 2011. Overall, the seasonal variations of P, Q, ET, air temperature and



354 vegetation parameters are similar in all TP basins with peak values occurred in May to
355 September (Fig.5 and Fig.6). The seasonal cycles of snow cover and SWE are
356 generally time consistent as well for 18 TP basins (the peak values mainly occur from
357 October to next April, Fig.7). With the ascending air temperature from cold to warm
358 months, the basin-wide precipitation increases and vegetation turns green gradually
359 (the basin-wide ET also increase). Meanwhile, glacier and snow melt or vanish
360 gradually with the melt water supply the river discharge together with precipitation.
361 The inter-basin variations of hydrological regime are to a large extent linked to the
362 climate systems that prevail over the TP.

363 [< Figure 5, here please, thanks >](#)

364 Although the temporal patterns of hydrological components are general analogous,
365 they varied among parameters, climate zones and even basins (Zhou et al., 2005). For
366 example, relative to air temperature, the seasonal variation of runoff is more similar to
367 precipitation which reveals that runoff is mainly controlled by precipitation in the TP
368 basins. It is in agreement with that summarized by Cuo et al. (2014). In the
369 westerlies-dominated basins, the peak values of precipitation and runoff mainly
370 concentrate in June-August, which contribute approximately 68-82% and 67-78% of
371 annual totals, respectively. During this period, the runoff always exceeds precipitation
372 which indicates large contributions of melt water to streamflow. It is consistent with
373 the existing findings in Tarim River (Yerqiang, Yulongkashi and Keliya rivers are the
374 major tributaries of Tarim River), which indicated that the melt water accounted for
375 about half of the annual total streamflow (Fu et al., 2008). The ET (vegetation cover)
376 in three westerlies-dominated basins are relatively less (scarcer) than that in other TP
377 basins while the percentages of glacier and seasonal snow cover are higher in these
378 basins which contribute more melt water to river discharge (Fig.6 and Fig.7). Overall,



379 the SWE in Yerqiang, Yulongkashi and Keliya rivers are relatively higher in winter
380 than other seasons, but they vary with basins and products which reveal considerable
381 uncertainties in SWE estimations.

382 [< Figure 6, here please, thanks >](#)

383 In the Indian monsoon and East Asian monsoon-dominated basins, the runoff
384 concentrates during June-September or June-October with precipitation being the
385 dominant contributor of annual total runoff. For example, the peak values of
386 precipitation and runoff occur during June-September at Zhimenda station
387 (contributing about 80% and 74% of the annual totals) while those occur during
388 June-October at Tangnaihahai station (contributing about 78% and 71% of the annual
389 totals, respectively). The results are quite similar to the related studies in eastern and
390 southern TP such as Liu (1999), Dong et al. (2007), Zhu et al. (2011), Zhang et al.
391 (2013), Cuo et al. (2014). The vegetation cover (ET) in most basins is relatively better
392 (higher) than that in the westerlies-dominant basins. Moreover, the seasonal snow
393 mainly covers from mid-autumn to spring and correspondingly the SWE is relatively
394 higher in these months in all basins except for Yellow River above Xining station,
395 Salwee River above Jiayuqiao station and Brahmaputra River above Nuxia and
396 Yangcun stations.

397 [< Figure 7, here please, thanks >](#)

398 **3.3 Trends of basin-wide water budget components for TP basins**

399 Trends in water budget components for 18 TP basins during the period 1982-2011
400 were also examined through the modified Mann-Kendall test (MMK) in this study.
401 The hydrological cycles intensified in the westerlies-dominated basins with Q, P and
402 ET_{wb} all ascended with regional warming (Fig.8), especially in the Keliya River
403 basin (Numaitilangan station). The aridity index (PET/P), which is an indicator for the



404 degree of dryness, declined in all basins in northwestern TP. The results were in line
405 with the overall climate warming and moistening reported in northwest China (Shi et
406 al., 2003), at which these basins located. The increase in streamflow was also found in
407 most tributaries of the Tarim River (Sun et al., 2006; Fu et al., 2010; Mamat et al.,
408 2010). Moreover, the westerlies, revealed by the Asian Zonal Circulation Index
409 (60° - 150° E), enhanced (linear trend: 0.21) over the period of 1982-2011 (Fig.9).
410 More water vapor was transported and fell as precipitation or snow in northwestern
411 TP (e.g., the eastern Pamir region) with the strengthening westerlies. The SWE
412 showed increase for all basins and for both products (VIC_IGSNRR simulated and
413 GlobaSnow-2 product) with the incremental seasonal snow cover and advanced
414 glaciers (Yao et al., 2012). More precipitation was transformed into snow or glacier
415 and the runoff coefficient (Q/P) exhibited decrease although precipitation obviously
416 increased (Fig.8). In addition, the transpiration in these basins may decrease with
417 vegetation degradation revealed by the NDVI and LAI (Yin et al., 2016) but the
418 atmospheric evaporative demand indicated by CRU PET increased (significantly
419 increase in the Yulongkashi and Keliya rivers) during the period 1982-2011.

420 [< Figure 8, here please, thanks >](#)

421 [< Figure 9, here please, thanks >](#)

422 In the East Asian monsoon-dominated basins, there are two types of change for
423 basin-wide water budget components. For example, P and Q decreased in the upper
424 Yellow River (Tangnihai, Huangheyuan and Jimai stations) and Yalong River (Yajiang
425 station) but increased in other basins (Zelingou, Gandatan, Xining, Tongren and
426 Zhimenda stations) over the period of 1982-2011 (Fig.10). The decline in Q and P for
427 the upper Yellow and Yalong Rivers (locate at eastern Tibetan Plateau) were
428 consistent with that found by Cuo et al. (2013, 2014) as well as Yang et al. (2014), and



429 were in line with the weakening (linear slope: -0.01) of the East Asian Summer
430 Monsoon (Fig.9). The vegetation turned green while ET_{wb} and PET increased in all
431 nine basins with the ascending air temperature during the period 1982-2011. The
432 aridity index (PET/P) was found decrease in all basins except for the upper Yellow
433 River basin above Jimai station and the upper Yalong River basin above Yajiang
434 station. Moreover, the runoff coefficients (SWE) were decrease (decrease except for
435 the Bayin River above Zelingou station and the upper Yellow River above Tongren
436 station) in the East Asian monsoon dominated basins.

437 [< Figure 10, here please, thanks >](#)

438 The hydrological cycles were also found intensified in the Indian monsoon-dominated
439 basins such as Salween River and Brahmaputra River (Fig.11), which were in line
440 with the strengthen (linear trend: 0.0006) of the Indian Summer monsoon (revealed by
441 the Indian Ocean Dipole Mode Index) during the specific period 1982-2011 (Fig.9).
442 In the six basins, trends in P, Q and ET_{wb} were all upward. For example, at
443 Jiayuqiao station, the annual streamflow showed increasing trend which was
444 consistent with that examined during 1980-2000 by Yao et al. (2012). The vegetation
445 status, revealed by NDVI and LAI, turned better with the ascending air temperature.
446 The aridity index (PET/P) decreased in all basins except for the Brahmaputra River
447 above Tangjia station, which indicated that most basins in the Indian
448 monsoon-dominated regions turn wet over the period of 1982-2011. The runoff
449 coefficient (Q/P) increased at Gongbujiangda and Nuxia while decreased at Jiayuqiao,
450 Pangduo, Tangji and Yangcun stations. Moreover, the basin-wide SWE declined in the
451 upper Salween River and Brahmaputra River above Pangduo, Tangjia and
452 Gongbujiangda stations while increased in Brahmaputra River above Nuxia and
453 Yangcun stations.



454 [< Figure 11, here please, thanks >](#)

455 **3.4 Uncertainties**

456 The results may unavoidably associate with several aspects of uncertainties which
457 mainly inherited from the multi-source datasets used. For example, although the
458 seasonal cycles of ET_{wb} can be captured by GLEAM_E and VIC_E, they still have
459 considerable uncertainties such as at Numaitilangan, Gongbujiangda and Nuxia
460 stations (Fig.5). With respect to the annual trend of ET_{wb} (Table 4), most ET products
461 (including the well-performed GLEAM_E and VIC_E in some basins) cannot detect
462 the decreasing trends in 7 out of 18 basins (at Kulukelangan, Tongguziluoke, Xining,
463 Tongren, Jimai, Nuxia and Gongbujiangda stations). We thus only used ET_{wb} in the
464 trend detection of water budget components in Fig.8, Fig.10 and Fig.11 in this study.
465 The two SWE products also showed large uncertainty, with respect to both their
466 seasonal cycles and trends due to their different forcing data; different algorithms
467 applied as well as varied spatial-temporal resolutions. Moreover, the interpolation of
468 missing values of runoff with VIC_IGSNRR simulated runoff and the gridded
469 precipitation data (which interpolated from limited gauged precipitation over the
470 plateau) involved some uncertainties as well as. However, with these caveats, we can
471 interpret the general hydrological regimes and their responses to the changing climate
472 in TP basins from solely the perspective of multi-source datasets, which are
473 comparable to the existing studies based on the in situ observations and complex
474 hydrological modeling.

475 [<Table 4, here please, thanks >](#)

476 **4 Summary**

477 In this study, we investigated the seasonal cycles and trends of water budget
478 components in 18 TP basins during the period 1982-2011, which is not well



479 understood so far due to the lack of adequate observations in the harsh environment,
480 through integrating the multi-source global/regional datasets such as gauge data,
481 satellite remote sensing and land surface model simulations. By using a two-step bias
482 correction procedure, annual basin-wide ET_{wb} was calculated through the water
483 balance considering the impacts of glacier and water storage change. The GLEAM_E
484 and VIC_E were found perform better relative to other products against the
485 calculated ET_{wb} .

486

487 The general water and energy budgets were different in the westerlies-dominated
488 (with higher aridity index, runoff coefficient and glacier cover), the Indian
489 monsoon-dominated and the East Asian monsoon-dominated (with higher air
490 temperature, vegetation cover and evapotranspiration) basins under the perspective of
491 Budyko framework. In 18 TP basins, precipitation is the major contributor to the river
492 runoff, which concentrates mainly during June-October (June-August for the
493 westerlies-dominated basins, June-September or June to October for the Indian
494 monsoon-dominated and the East Asian monsoon-dominated basins). The basin-wide
495 SWE is relatively higher from mid-autumn to spring for all 18 TP basins except for
496 Keliya River and Brahmaputra River above the Nuxia and Yangcun stations. The
497 vegetation cover is relatively less whereas snow/glacier cover is more in the
498 westerlies-dominant basins compared with other basins. The hydrological cycles were
499 found intensified under the regional warming in most TP basins except for most
500 tributaries of the upper Yellow River and the Yalong River, which were significantly
501 influenced by the weakening East Asian monsoon during the period 1982-2011. The
502 aridity index (PET/P) exhibited decrease in most TP basins which corresponded to the
503 warming and moistening climate in the TP and western China. Moreover, the runoff



504 coefficient (Q/P) declined in most basins which may be, to some extent, due to ET
505 increase induced by vegetation greening and the influences of snow and glacier
506 changes. Although there are considerable uncertainties inherited from multi-source
507 data used, the general hydrological regimes in TP basins could be revealed, which are
508 consistent to the existing results obtained from in situ observations and complex land
509 surface modeling. It indicated the usefulness of integrating the multiple datasets
510 available such as in situ observations, remote sensing-based products, reanalysis
511 outputs, land surface model simulations and climate model outputs for hydrological
512 applications. The results obtained could be helpful for understanding the hydrological
513 cycles, and further for the water resources management and eco-environment
514 protection under a warming climate in the vulnerable Tibetan Plateau.

515

516 **Author contributions.** Wenbin Liu and Fubao Sun developed the idea to see the
517 general water budgets in TP basins from the perspective of multisource datasets.
518 Wenbin Liu collected and processed the multiple datasets with the help of Yanzhong
519 Li, Guoqing Zhang, Hong Wang as well as Peng Bai, and prepared the manuscript.
520 The results were extensively commented and discussed by Fubao Sun, Jiahong Liu
521 and Yan-Fang Sang.

522

523 **Acknowledgements.** This study was supported by the National Key Research and
524 Development Program of China (2016YFC0401401 and 2016YFA0602402), National
525 Natural Science Foundation of China (41401037 and 41330529), the Open Research
526 Fund of State Key Laboratory of Desert and Oasis Ecology in Xinjiang Institute of
527 Ecology and Geography, Chinese Academy of Sciences (CAS), the CAS Pioneer
528 Hundred Talents Program (Fubao Sun), the Initial Founding of Scientific Research
529 (Y5V50019YE) and the program for the “Bingwei” Excellent Talents from the



530 Institute of Geographic Sciences and Natural Resources Research, CAS. We are
531 grateful to the NASA MEaSUREs Program (Sean Swenson) for providing the
532 GRACE land data processing algorithm. The basin-wide water budget series in TP
533 Rivers used in this study are available from the authors upon request
534 (liuwb@igsnr.ac.cn).

535

536 **References**

537 Akhtar, M., Ahmad, N., and Booij, M.J.: Use of regional climate model simulations as input for
538 hydrological models for the Hindukush-Karakorum-Himalaya region, Hydrol. Earth Syst. Sci.
539 13, 1075-1089, 2009.

540 Bai, P., Liu, X.M., Yang, T.T., Liang, K., and Liu, C.M.: Evaluation of streamflow simulation
541 results of land surface models in GLDAS on the Tibetan Plateau, J. Geophys. Res. Atmos., 121,
542 12180-12197, 2016.

543 Berrisford, P, Lee, D., Poli, P., Brugge, R., Fielding, K., Fuentes, M., Kallberg, P., Kobayashi, S.,
544 Uppala, S., and Simmons, A.: The ERA-interim archive. ERA Reports Series No. 1 Version 2.0,
545 Available from: [https://www.researchgate.net/publication/41571692_The_ERA-interim](https://www.researchgate.net/publication/41571692_The_ERA-interim_archive)
546 archive>, 2011.

547 Bookhagen, B. and Burbank, D.W.: Toward a complete Himalayan hydrological budget:
548 spatiotemporal distribution of snowmelt and rainfall and their impact on river discharge, J.
549 Geophys. Res., 115, F03019, 2010.

550 Bouraoui, F., Vachaud, G., Li, L.Z.X., LeTreut, H., and Chen, T.: Evaluation of the impact of
551 climate changes on water storage and groundwater recharge at the watershed scale, Clim. Dyn.,
552 15(2), 153-161, 1999.

553 Budyko, M.I.: Climate and life. Academic Press, 1974.

554 Chen, D., Xu, B., Yao, T., Guo, Z., Cui, P., Chen, F., Zhang, R., Zhang, X., Zhang, Y., Fan, J., Hou,
555 Z., and Zhang, T.: Assessment of past, present and future environmental changes on the Tibetan
556 Plateau, Chinese SCI. Bull., 60(32), 3025-3035, 2015 (in Chinese).

557 Chen, J.: Lichenometrical studies on glacier changes during the Holocene Epoch at the sources



- 558 region of Urumqi River, *Sci. China B.*, 18(1), 95-104, 1988 (in Chinese).
- 559 Cuo, L., Zhang, Y.X., Bohn, T.J., Zhao, L., Li, J.L., Liu, Q.M., and Zhou, B.R.: Frozen soil
560 degradation and its effects on surface hydrology in the northern Tibetan Plateau, *J. Geophys.*
561 *Res. Atmos.*, 120(6), 8276-8298, 2015.
- 562 Cuo, L., Zhang, Y.X., Gao, Y., Hao, Z., and Cairang, L.: The impacts of climate change and land
563 cover/use transition on the hydrology in the upper Yellow River Basin, China, *J. Hydrol.*, 502,
564 37-52, 2013.
- 565 Cuo, L., Zhang, Y.X., Zhu, F.X., and Liang, L.Q.: Characteristics and changes of streamflow on
566 the Tibetan Plateau: A review, *J. Hydrol. Reg. stud.*, 2, 49-68, 2014.
- 567 Dong, X., Yao, Z., and Chen, C.: Runoff variation and responses to precipitation in the source
568 regions of the Yellow River, *Resour. Sci.*, 29(3), 67-73, 2007 (in Chinese).
- 569 Duan, A.M. and Wu, G.X.: Change of cloud amount and the climate warming on the Tibetan
570 Plateau, *Geophys. Res. Lett.*, 33, L22704, 2006.
- 571 Fu, L., Chen, Y., Li, W., Xu, C., and He, B.: Influence of climate change on runoff and water
572 resources in the headwaters of the Tarim River, *Arid Land Geogr.*, 31(2), 237-242, 2008 (in
573 Chinese).
- 574 Fu, L., Chen, Y., Li, W., He, B., and Xu, C.: Relation between climate change and runoff volume
575 in the headwaters of the Tarim River during the last 50 years., *J. Desert Res.*, 30(1), 204-209,
576 2010 (in Chinese).
- 577 Guo, W.Q., Liu, S.Y., Yao, X.J., Xu, J.L., Shangguan, D.H., Wu, L.Z., Zhao, J.D., Liu, Q., Jiang,
578 Z.L., Wei, J.F., Bao, E.J., Yu, P.C., Ding, L.F., Li, G., Ge, C.M., and Wang, Y.: The Second
579 Glacier Inventory Dataset of China, Cold and Arid Regions Science Data Center at Lanzhou,
580 doi: 10.3972/glacier.001.2013.db, 2014.
- 581 Hamed, K.H. and Rao, A.R.: A modified Mann-Kendall trend test for autocorrelation data,
582 *J. Hydrol.*, 204(1-4), 182-196, 1998.
- 583 Huffman, G.J., , E.F., Bolvin, D.T., Nelkin, E.J., and Adler, R.F.: last updated 2013: TRMM
584 Version 7 3B42 and 3B43 Data Sets, NASA/GSFC, Greenbelt, MD. Data set accessed at
585 <http://mirador.gsfc.nasa.gov/cgi-bin/mirador/>



- 586 presentNavigation.pl?tree=project&project=TRMM&dataGroup=Gridded&CGIS
- 587 ESSID=5d12e2ffa38ca2aac6262202a79d882a, 2012.
- 588 Harris, I., Jones, P.D., Osborn, T.J., and Lister, D.H.: Updated high-resolution grids of monthly
589 climatic observations – the CRU TS3.10 Dataset, *Int. J. Climatol.*, 34 (3), 623-642, 2014.
- 590 Immerzeel, W.W., van Beek, L.P.H., and Bierkens, M.F.P.: Climate change will affect the Asian
591 water towers, *Science*, 328, 1382-1385, 2010.
- 592 Jung, M., Reichstein, M., Ciais, P., Seneviratne, S.I., Sheffield, J., Goulden, M.L., Bonan, G.,
593 Cescatti, A., Chen, J., de Jeu, R., Dolman, A.J., Eugster, W., Gerten, D., Gianelle, D., Gobron, N.,
594 Heinke, J., Kimball, J., Law, B.E., Montagnani, L., Mu, Q., Mueller, B., Oleson, K., Papale, D.,
595 Richardson, A.D., Rouspard, O., Running, S., Tomelleri, E., Viovy, N., Weber, U., Williams, C.,
596 Wood, E., Zaehle, S., and Zhang, K.: Recent decline in the global land evapotranspiration trend
597 due to limited moisture supply, *Nature*, 467, 951-954, 2010.
- 598 Kobayashi, S., Ota, Y., Harada, Y., Ebata, A., Moriya, M., Onoda, H., Onogi, K., kamahori, H.,
599 kobayashi, C., Endo, H., miyaoka, K., and Takahashi, K.: The JRA-55 Reanalysis: General
600 specifications and basic characteristics, *J.Meteor. Soc. Japan*, 93(1), 5-58, doi:
601 10.2151/jmsj.2015-001, 2015.
- 602 Landerer, F.W. and Swenson, S.C.: Accuracy of scaled GRACE terrestrial water storage estimates,
603 *Water Resour.Res.*, 48, W04531, 2012.
- 604 Li, F.P., Zhang, Y.Q., Xu, Z.X., Liu, C.M., Zhou, Y.C., and Liu, W.F.: Runoff predictions in
605 ungauged catchments in southeast Tibetan Plateau, *J. Hydrol.*, 511, 28-38, 2014.
- 606 Li, F.P., Zhang, Y.Q., Xu, Z.X., Teng, J., Liu, C.M., Liu, W.F., and Mpelasoka, F.: The impact of
607 climate change on runoff in the southeastern Tibetan Plateau, *J. Hydrol.*, 505, 188-201, 2013.
- 608 Li, J.P. and Zeng, Q.C.: A unified monsoon index, *Geophys. Res. Lett.*, 29(8), 1274, 2002.
- 609 Li, X.P., Wang, L., Chen, D.L., Yang, K., and Wang, A.H.: Seasonal evapotranspiration changes
610 (1983-2006) of four large basins on the Tibetan Plateau, *J. Geophys. Res.*, 119 (23),
611 13079-13095, 2014.
- 612 Liang, S.L. and Xiao, Z.Q.: Global Land Surface Products: Leaf Area Index Product Data
613 Collection(1985-2010), Beijing Normal University, doi:10.6050/glass863.3004.db, 2012.



- 614 Liu, J., Liu, T., Bao, A., De Maeyer, P., Feng, X., Miller, S.N., and Chen, X.: Assessment of
615 different modeling studies on the spatial hydrological processes in an arid alpine catchment,
616 *Water Resour. Manag.*, 30, 1757-1770, 2016.
- 617 Liu, T.: Hydrological characteristics of Yalungzangbo River, *Acta Geogr. Sin.*, 54 (Suppl.),
618 157-164, 1999 (in Chinese).
- 619 Liu, W.B. and Sun, F.B.: Assessing estimates of evaporative demand in climate models using
620 observed pan evaporation over China, *J. Geophys. Res. Atmos.*, 121, 8329-8349, 2016.
- 621 Liu, W.B., Wang, L., Zhou, J., Li, Y.Z., Sun, F.B., Fu, G.B., Li, X.P., and Sang, Y-F.: A worldwide
622 evaluation of basin-scale evapotranspiration estimates against the water balance method, *J.*
623 *Hydrol.*, 538, 82-95, 2016a.
- 624 Liu, W.B., Wang, L., Chen, D.L., Tu, K., Ruan, C.Q., and Hu, Z.Y.: Large-scale circulation
625 classification and its links to observed precipitation in the eastern and central Tibetan Plateau,
626 *Clim. Dyn.*, 46, 3481-3497, 2016b.
- 627 Liu, X.M., Yang, T., Hsu, K., Liu, C., and Sorooshian, S.: Evaluating the streamflow simulation
628 capability of PERSIANN-CDR daily rainfall products in two river basins on the Tibetan Plateau,
629 *Hydrol. Earth Syst. Sci. Discuss.*, doi: 10.5194/hess-20160282, 2016.
- 630 Long, D., Shen, Y.J., Sun, A., Hong, Y., Longuevergne, L., Yang, Y.T., Li, B., and Chen, L.:
631 Drought and flood monitoring for a large karst plateau in Southwest China using extended
632 GRACE data, *Remote Sen. Environ.*, 155, 145-160, 2014.
- 633 Lucchesi, R.: File specification for MERRA products, GMAO Office Note No.1 (version 2.3), 82
634 pp, available from http://gmao.gsfc.nasa.gov/pubs/office_notes, 2012.
- 635 Ma, N., Szilagyi, J., Niu, G.Y., Zhang, Y.S., Zhang, T., Wang, B.B., and Wu, Y.H.: Evaporation
636 variability of Nam Co Lake in the Tibetan Plateau and its role in recent rapid lake expansion, *J.*
637 *Hydrol.*, 537, 27-35, 2016.
- 638 Ma, N., Zhang, Y.S., Guo, Y.H., Gao, H.F., Zhang, H.B., and Wang, Y.F.: Environmental and
639 biophysical controls on the evapotranspiration over the highest alpine steppe, *J. Hydrol.*, 529,
640 980-992, 2015.



- 641 Mamat, A., Halik, W., and Yang, X.: The climatic changes of Qarqan river basin and its impact on
642 the runoff, *Xinjiang Agric. Sci.*, 47 (5), 996-1001, 2010 (in Chinese).
- 643 Mansur, S. and Ajinisa, T.: An analysis of water resources and it's hydrological characteristics of
644 Yarkend River Valley, *J. Xinjiang Norm. Univ. (Nat. Sci. Ed.)*, 24(1), 74-78, 2005 (in Chinese).
- 645 McVicar, T.R., Roderick, M., Donohue, R.J., Li, L.T., Van Niel, T.G., Thomas, A., Grieser, J.,
646 Jhajharia, D., Himri, Y., Mahowald, N.M., Mescherskaya, A.V., Kruger, A.C., Rehman, S., and
647 Dinpashoh, Y.: Global review and synthesis of trends in observed terrestrial near-surface wind
648 speeds: implications for evaporation, *J. Hydrol.*, 416-417, 182-205, 2012.
- 649 Miralles, D.G., De Jeu, R.A.M., Gash, J.H., Holmes, T.R.H., and Dolman, A.J.: Magnitude and
650 variability of land evaporation and its components at the global scale, *Hydrol. Earth Syst. Sci.*, 15,
651 967-981, 2011.
- 652 Miralles, D.G., Gash, J.H., Holmes, T.R.H., de Jeu, R.A.M, and Dolman, A.J.: Global canopy
653 interception from satellite observations, *J. Geophys. Res.*, 115, D16122, 2010.
- 654 Neckel, N., Kropáček, J., Bolch, T., and Hochschild, V.: Glacier mass changes on the Tibetan
655 Plateau 2003-2009 derived from ICESat laser altimetry measurements, *Environ. Res. Lett.*, 9,
656 014009(7pp), 2014.
- 657 Oliveira, P.T.S., Mearing, M.A., Moran, M.S., Goodrich, D.C., Wendland, E., and Gupta, H.V.:
658 Trends in water balance components across the Brazilian Cerrado, *Water Resour. Res.*, 50,
659 7100-7114, 2014.
- 660 Rodell, M., Houser, P.R., Jambor, U., Gottschalck, J., Mitchell, K., Meng, C.-J., Arsenault, K.,
661 Cosgrove, B., Radakovich, J., Bosilovich, M., Entin, J.K., Walker, P., Lohmann, D., and Toll, D.:
662 The global land data assimilation system, *B. Am. Meteorol. Soc.*, 85, 381-394, 2004.
- 663 Rui, H.: README Document for Global Land Data Assimilation System Version 2 (GLDAS-2)
664 Products, GES DISC, 2011.
- 665 Saji, N.H., Goswami, B.N., Vinayachandran, P.N., and Yamagata, T.: A dipole mode in the tropical
666 Indian Ocean, *Nature*, 401, 360-363, 1999.
- 667 Shi, Y.F., Shen, Y.P., Li, D.L., Zhang, G.W., Ding, Y.J., Hu, R.J., and Kang, E.S.: Discussion on
668 the present climate change from Warm2dry to Warm2wet in northwest China, *Quat. Sci.*, 23(2),
669 152-164, 2003 (in Chinese).
- 670 Shepard, D.S.: Computer mapping: the SYMAP interpolation algorithm. *Spatial Statistics and*
27 / 51



- 671 Models, G.L. Gaile and C.J. Willmott, Eds., D. Reidel, 133-145, 1984.
- 672 Sun, B., Mao, W., Feng, Y., Chang, T., Zhang, L., and Zhao, L.: Study on the change of air
673 temperature, precipitation and runoff volume in the Yarkant River basin, *Arid Zone Res.*, 23(2),
674 203-209, 2006 (in Chinese).
- 675 Takala, M., Luoju, K., Pulliainen, J., Derksen, C., Lemmetyinen, J., Kärnä, J.-P., Koskinen, J., and
676 Bojkov, B.: Estimating northern hemisphere snow water equivalent for climate research through
677 assimilation of spaceborne radiometer data and ground-based measurements, *Remote
678 Sens. Environ.*, 115 (12), 3517-3529, 2011.
- 679 Tapley, B.D., Bettadpur, S., Watkins, M., and Reigber, C.: The gravity recovery and climate
680 experiment: mission overview and early results, *Geophys. Res. Lett.*, 31, L09607, 2004.
- 681 Tian, L., Yao, T., MacClune, K., White, J.W.C., Schilla, A., Vaughn, B., Vachon, R., and
682 Ichiyangi, K.: Stable isotopic variations in west China: a consideration of moisture sources, *J.
683 Geophys. Res. Atmos.*, 112, D10112, 2007.
- 684 Tucker, C.J., Pinzon, J.E., Brown, M.E., Slayback, D., Pak, E.W., Mahoney, R., Vermote, E., and
685 El Saleous, N.: An extended AVHRR 8 km NDVI data set compatible with MODIS and SPOT
686 vegetation NDVI data, *Int. J. Remote Sens.*, 26(20), 4485-4498, 2005.
- 687 Wang, A. and Zeng, X.: Evaluation of multireanalysis products within site observations over the
688 Tibetan Plateau, *J. Geophys. Res.*, 117, D05102, 2012.
- 689 Wang, L., Sun, L.T., Shrestha, M., Li, X.P., Liu, W.B., Zhou, J., Yang, K., Lu, H., and Chen, D.L.:
690 Improving snow process modeling with satellite-based estimation of
691 near-surface-air-temperature lapse rate, *J. Geophys. Res. Atmos.*, 121, 12005-12030, 2016.
- 692 Xia, Y., Mitchell, K., Ek, M., Cosgrove, B., Sheffield, J., Luo, L., Alonge, C., Wei, H., Meng, J.,
693 Livneh, B., and Duang, Q.: Continental-scale water and energy flux analysis and validation for
694 North American Land Data Assimilation System project phase 2 (NLDAS-2): 2. Validation of
695 model-simulated streamflow, *J. Geophys. Res. Atmos.*, 117(D3), D03110, 2012.
- 696 Xu, L.: The land surface water and energy budgets over the Tibetan Plateau, Available from
697 Nature Precedings < <http://hdl.handle.net/10101/npre.2011.5587.1>>, 2011.
- 698 Xue, B.L., Wang, L., Yang, K., Tian, L., Qin, J., Chen, Y., Zhao, L., Ma, Y., Koike, T., Hu, Z., and



- 699 Li, X.P.: Modeling the land surface water and energy cycle of a mesoscale watershed in the
700 central Tibetan Plateau with a distributed hydrological model, *J. Geophys. Res. Atmos.*, 118,
701 8857-8868, 2013.
- 702 Yao, Z., Duan, R., and Liu, Z.: Changes in precipitation and air temperature and its impacts on
703 runoff in the Nujiang River basins. *Resour. Sci.* 34(2), 202-210, 2012 (in Chinese)
- 704 Yang, K., Qin, J., Zhao, L., Chen, Y.Y., Tang, W.J., Han, M.L., Lazhu, Chen, Z.Q., Lv, N., Ding,
705 B.H., Wu, H., and Lin, C.G.: A multi-scale soil moisture and freeze-thaw monitoring network
706 on the third pole, *Bull. Am. Meteorol. Soc.*, 94,1907-1916, 2013.
- 707 Yang, K., Wu, H., Qin, J., Lin, C.G., Tang, W.J., and Chen, Y.Y.: Recent climate changes over the
708 Tibetan Plateau and their impacts on energy and water cycle: a review, *Glob. Planet Change*,
709 112, 79-91, 2014.
- 710 Yao, T.D., Thompson, L., Yang, W., Yu, W.S., Gao, Y., Guo, X.J., Yang, X.X., Duan, K.Q., Zhao,
711 H.B., Xu, B.Q., Pu, J.C., Lu, A.X., Xiang, Y., Kattel, D.B., and Joswiak, D.: Different glacier
712 status with atmospheric circulations in Tibetan Plateau and surroundings, *Nat. Clim. Change*, 2,
713 1-5, 2012.
- 714 Yin, G., Hu, Z.Y., Chen, X., and Tiyip, T.: Vegetation dynamics and its response to climate change
715 in Central Asia, *J. Arid Land*, 8, 375, 2016.
- 716 Yu, J., Zhang, G., Yao, T., Xie, H., Zhang, H., Ke, C., and Yao, R.: Developing daily cloud-free
717 snow composite products from MODIS Terra-Aqua and IMS for the Tibetan Plateau, *IEEE*
718 *Trans. Geosci. Remote Sens.*, 54(4), 2171-2180, 2015.
- 719 Zhang, D., Liu, X., Zhang, Q., Liang, K., and Liu, C.: Investigation of factors affecting
720 inter-annual variability of evapotranspiration and streamflow under different climate conditions.
721 *J. Hydrol.*, doi:10.1016/j.jhydrol.2016.10.047, 2016.
- 722 Zhang, G., Xie, H., Yao, T., Liang, T., and Kang, S.: Snow cover dynamics of four lake basins
723 over Tibetan Plateau using time series MODIS data (2001-2100), *Water Resour. Res.*, 48(10),
724 W10529, 2012.
- 725 Zhang, K., Kimball, J.S., Nemani, R.R., and Running, S.W.: A continuous satellite-derived global
726 record of land surface evapotranspiration from 1983 to 2006, *Water Resour. Res.*, 46(9),
727 W09522, 2010.
- 728 Zhang, L., Su, F., Yang, D., Hao, Z., and Tong, K.: Discharge regime and simulation for the
29 / 51



- 729 upstream of major rivers over Tibetan Plateau, *J. Geophys. Res. Atmos.*, 118(15), 8500-8518,
730 2013.
- 731 Zhang, X., Tang, Q., Pan, M., and Tang, Y.: A long-term land surface hydrologic fluxes and states
732 dataset for China, *J. Hydrometeorol.*, 15, 2067-2084, 2014.
- 733 Zhang, Y., Peña-Arancibia, J.L., McVicar, T.R., Chiew, F.H.S., Vaze, J., Liu, C.M., Lu, X.J.,
734 Zheng, H.X., Wang, Y.P., Liu, Y.Y., Miralles, D.G., and Pan, M.: Multi-decadal trends in global
735 terrestrial evapotranspiration and its components, *Scientific Reports*, 6, 19124, 2016.
- 736 Zhang, Y., Liu, C., Tang, Y., and Yang, Y.: Trend in pan evaporation and reference and actual
737 evapotranspiration across the Tibetan Plateau, *J. Geophys. Res.*, 112, D12110, 2007.
- 738 Zhou, C., Jia, S., Yan, H., and Yang, G.: Changing trend of water resources in Qinghai Province
739 from 1956 to 2000, *J. Glaciol. Geocryol.*, 27(3), 432-437, 2005 (in Chinese).
- 740 Zhou, J., Wang, L., Zhang, Y.S., Guo, Y.H., Li, X.P., and Liu, W.B.: Exploring the water storage
741 changes in the largest lake (Selin Co) over the Tibetan Plateau during 2003-2012 from a
742 basin-wide hydrological modeling., *Water Resour. Res.*, 51, 8060-8086, 2015.
- 743 Zhou, S.Q., Kang, S., Chen, F., and Joswiak, D.R.: Water balance observations reveal significant
744 subsurface water seepage from Lake Nam Co., south-central Tibetan Plateau., *J. Hydrol.*, 491,
745 89-99, 2013.
- 746 Zhou, S.Q., Wang, Z., and Joswiak, D.R.: From precipitation to runoff: stable isotopic fractionation
747 effect of glacier melting on a catchment scale, *Hydrol. Process.*, 28(8), 3341-3349, 2014.
- 748 Zhu, Y., Chen, J., Chen, G.: Runoff variation and its impacting factors in the headwaters of the
749 Yangtze River in recent 32 years, *J. Yangtze River Sci. Res. Inst.*, 28(6), 1-4, 2011 (in Chinese).



750 **Table 1:** Main features of the 18 used TP river basins. GA% and SC% represent the percentages of multiyear-mean glacier cover and snow cover in each basin.
 751 The glacier and snow cover data are extracted, respectively, from the Second Glacier Inventory Dataset of China and the daily TP snow cover dataset
 752 (2005-2013)
 753

No.	Station	Altitude (m)	River name	Drainage area (km ²)	Multiyear-mean (1982-2011) and basin-averaged parameters						
					Q (mm/yr)	Prec. (mm/yr)	Temp.(°C/yr)	NDVI	LAI	GA%	SC%
01	Kulukelangan	2000	Yerqiang	32880.00	158.60	128.34	-5.68	0.05	0.03	10.97	35.03
02	Tongguziluoke	1650	Yulongkashi	14575.00	151.56	134.04	-4.07	0.06	0.04	23.27	35.95
03	Numaitilangan	1880	Keliya	7358.00	103.18	137.14	-4.78	0.06	0.03	10.86	29.16
04	Zelingou	4282	Bayin	5544.00	41.42	340.68	-4.98	0.13	0.09	0.09	21.22
05	Gadatan	3823	Yellow	7893.00	200.95	566.01	-4.60	0.34	0.54	0.13	14.94
06	Ximing	3225	Yellow	9022.00	99.90	503.74	0.97	0.36	0.70	0.00	10.06
07	Tongren	3697	Yellow	2832.00	149.36	533.25	-1.37	0.39	0.83	0.00	9.42
08	Tainaihai	2632	Yellow	121972.00	159.48	540.32	-2.40	0.34	0.72	0.09	15.89
09	Huangheyuan	4491	Yellow	20930.00	31.18	386.42	-4.81	0.23	0.61	0.00	17.25
10	Jimai	4450	Yellow	45015.00	85.50	441.48	-4.16	0.26	0.52	0.00	20.05
11	Yajiang	2599	Yalong	67514.00	237.66	717.05	-0.23	0.43	0.80	0.15	18.36
12	Zhimenda	3540	Yangtze	137704.00	96.23	405.66	-4.83	0.20	0.26	0.96	17.87
13	Jiaoyuqiao	3000	Salween	72844.00	364.26	620.88	-1.89	0.29	0.44	2.02	23.73
14	Pangduo	5015	Brahmaputra	16459.00	348.31	544.59	-1.53	0.27	0.33	1.66	23.33
15	Tangjia	4982	Brahmaputra	20143.00	350.61	555.17	-1.89	0.27	0.34	1.39	21.83
16	Gongbuijiangda	4927	Brahmaputra	6417.00	586.96	692.06	-4.24	0.27	0.36	4.12	25.99
17	Nuxia	2910	Brahmaputra	191235.00	307.38	401.35	-0.73	0.22	0.25	1.90	13.50
18	Yangcun	3600	Brahmaputra	152701.00	163.25	349.91	-0.87	0.19	0.18	1.28	10.52



Table 2: Overview of multi-source datasets applied in this study

Data category	Data source	Spatial resolution	Temporal resolution	Available period used	Reference
Runoff (Q)	Observed, National Hydrology Almanac of China	—	Daily	1982-2011	—
Precipitation (P)	VIC_IGSNRRR simulated	0.25°	Daily	1982-2011	Zhang et al. (2014)
	Observed, CMA	0.5°	Monthly	1982-2011	—
	TRMM 3B43 V7	0.25°	Monthly	2000-2011	Huffman et al. (2012)
	IGSNRRR forcing	0.25°	Daily	1982-2011	Zhang et al. (2014)
Temperature (Temp.)	Observed, CMA	0.5°	Monthly	2000-2011	—
Terrestrial storage change (ΔS)	GRACE-CSR	Approx.300-400 km	Monthly	2002-2011	Tapley et al. (2004)
	GRACE-GFZ	Approx.300-400 km	Monthly	2002-2011	Tapley et al. (2004)
	GRACE-JPL	Approx.300-400 km	Monthly	2002-2011	Tapley et al. (2004)
Potential evaporation (PET)	CRU	0.5°	Monthly	1982-2011	Harris et al. (2013)
Actual evaporation (ET)	MTE_E	0.5°	Monthly	1982-2011	Jung et al. (2010)
	VIC_E	0.25°	Daily	1982-2011	Zhang et al. (2014)
NDVI	GLEAM_E	0.25°	Daily	1982-2011	Miralles et al. (2011)
	PML_E	0.5°	Monthly	1982-2011	Zhang Y et al. (2016)
	Zhang_E	8 km	Monthly	1983-2006	Zhang et al. (2010)
	GNoah_E	1.0°	3 hourly	1982-2011	Rui (2011)
LAI	GIMMS NDVI dataset	8 km	15 daily	1982-2011	Tucker et al. (2005)
	GLASS LAI Product	0.05°	8 daily	1982-2011	Liang and Xiao (2012)
Snow Cover	TP Snow composite Products	500 m	Daily	2005-2013	Zhang et al. (2012)
SWE	VIC_IGSNRRR simulated	0.25°	Daily	1982-2011	Zhang et al. (2014)
	GlobSnow-2 Product	25 km	Daily	1982-2011	Takala et al. (2011)



759 **Table 3:** Contribution of glacier-melt to discharge in eighteen basins (“—” shows no glacier influences, “—*” shows the percentage is empirically estimated
 760 through the relation between glacier area ratio and glacier melt for basins in which the glacier melt contribution has been reported in existing studies)
 761

Basin	Contributions of glacier-melt to discharge (%)	Reference
Kulkelangan	62.73	Mansur and Ajnisa (2005)
Tongguziluoke	64.90	Liu J et al. (2016)
Numaitilangan	71	Chen (1988)
Zelingou	—	—
Gadatan	—	—
Ximing	—	—
Tongren	—	—
Tainathai	0.80	Zhang et al. (2013)
Huangheyuan	—	—
Jimai	—	—
Yajiang	1.40	—*
Zhimenda	6.50	Zhang et al. (2013)
Jiaoyuqiao	4.80	Zhang et al. (2013)
Nuxia	11.60	Zhang et al. (2013)
Pangduo	10.13	—*
Tangjia	8.49	—*
Gongbujiangda	25.15	—*
Yangcun	7.81	—*



Table 4: Nonparametric trends for different ET estimates during the period 1982–2006 detected by modified Mann-Kendall test, the bold number showed the detected trend is statistically significant at the 0.05 level

Basin	ET _{wb}	GLEAM_E	VIC_E	Zhang_E	PML_E	MET_E	GNoah_E
Kulukelangan	-0.09	0.09	0.18	–	0.03	-0.01	0.07
Tongguziluoke	-0.02	0.10	0.13	–	0.03	-0.08	0.19
Numaitilangan	0.04	0.10	0.14	–	0.14	-0.10	0.22
Zelingou	0.13	0.23	0.11	0.09	0.04	0.06	0.02
Gadatan	-0.09	0.25	0.070	-0.10	-0.01	0.06	-0.07
Xining	-0.06	0.54	0.01	-0.08	0.01	0.02	-0.06
Tongren	-0.06	0.34	-0.15	-0.17	0.07	0.02	0.13
Taimathai	0.06	0.28	-0.03	-0.11	0.04	0.05	0.04
Huangheyan	0.08	0.19	-0.01	-0.10	0.08	0.05	0.10
Jimai	-0.07	0.23	-0.01	-0.08	0.03	0.05	0.10
Yajiang	0.17	0.26	0.06	-0.21	-0.01	0.03	-0.02
Zhimenda	0.11	0.28	0.10	0.01	0.07	0.04	0.07
Jiaoyuqiao	0.18	0.28	0.10	-0.11	0.05	0.05	0.07
Nuxia	-0.09	0.25	0.09	-0.10	0.12	0.04	0.10
Pangduo	0.05	0.28	0.17	-0.07	0.07	0.07	0.11
Tangjia	0.09	0.26	0.17	-0.09	0.20	0.06	0.12
Gongbujiangda	-0.26	0.12	0.13	-0.16	0.19	0.01	0.15
Yangcun	0.03	0.28	0.08	-0.06	0.10	0.04	0.09



780 **Figure captions:**

781 **Figure 1.** Map of river basins and hydrological gauging stations (green dots) over the
782 Tibetan Plateau (TP) used in this study. The grey shading shows the topography of TP
783 in meters above the sea level and the blue shading exhibits the glaciers distribution in
784 TP extracted from the Second Glacier Inventory Dataset of China.

785 **Figure 2.** Comparison of VIC_IGSNRR simulated and observed monthly runoff for
786 Tangnaihai and Panduo stations (a and b) as well as (c) basin-averaged monthly
787 TRMM, CMA gridded and IGSNRR forcing precipitations for the smallest basin
788 (Tongren station) over the period 1982-2011. (d) shows the comparison of TRMM
789 (blue) and IGSNRR forcing (red) precipitations against CMA gridded precipitation for
790 18 river basins over TP during the period 2000-2011.

791 **Figure 3.** Comparison of different ET products against the calculated ET through the
792 water balance method (ET_{wb}) for 18 TP basins. The boxplot of annual estimates of
793 different ET products for 18 TP basins are shown in (a) while the correlation
794 coefficients and root-mean-square-errors (RMSEs, mm/month) for each ET product
795 relatively to ET_{wb} are exhibited in (b).

796 **Figure 4.** General water and energy status (a. the perspective of Budyko framework)
797 and their relationships with glacier (b) and vegetation (c and d) for eighteen TP river
798 basins (1983-2006). The ET used in this figure is calculated from the bias-corrected
799 water balance method.

800 **Figure 5.** Seasonal cycles (1982-2011) of water budget components in westerlies-
801 dominated (column 1), East Asian monsoon-dominated (columns 2-4) and Indian
802 monsoon-dominated (columns 5-6) TP basins.

803 **Figure 6.** Seasonal cycles (1982-2011) of air temperature and vegetation parameters
804 in westerlies-dominated (column 1), East Asian monsoon-dominated (columns 2-4)
805 and Indian monsoon-dominated (columns 5-6) TP basins.

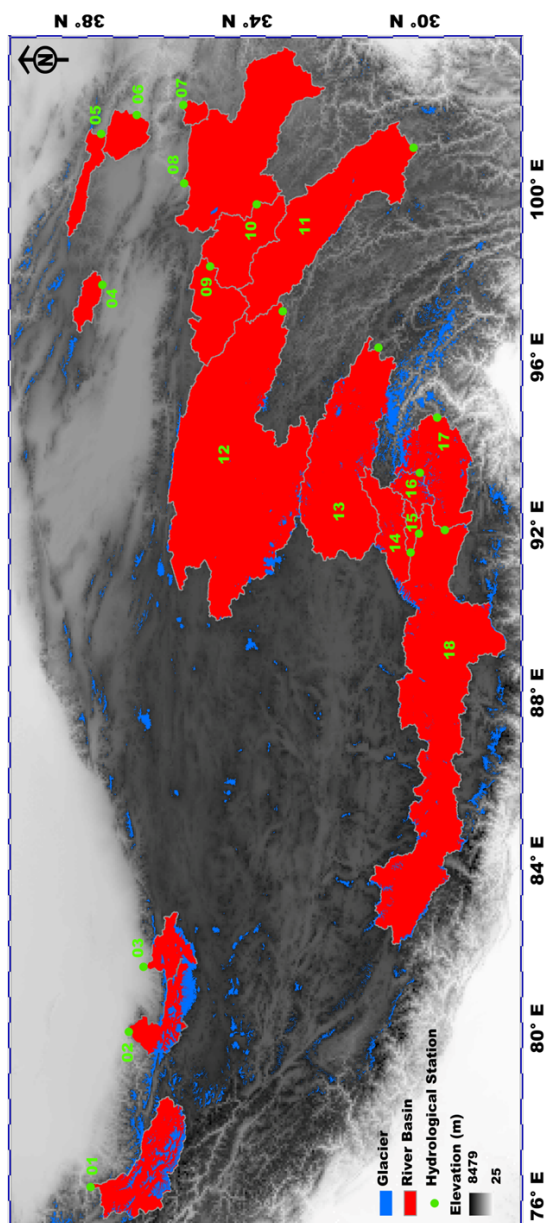
806 **Figure 7.** Seasonal cycles (1982-2011) of snow cover and snow water equivalent
807 (SWE) in westerlies-dominated (column 1), East Asian monsoon-dominated (columns
808 2-4) and Indian monsoon-dominated (columns 5-6) TP basins. The snow cover was



809 extracted from cloud free snow composite product during the period 2005-2013. It
810 should also be noted that the GlobSnow data are not available for some basins.
811 **Figure 8.** Sen's slopes of water budget components and vegetation parameters in
812 westerlies-dominated TP basins during the period of 1982-2011. The double red stars
813 showed that the trend was statistically significant at the 0.05 level.
814 **Figure 9.** Linear trends of westerly, Indian monsoon and East Asian summer monsoon
815 during the period 1982-2011 revealed prospectively by the Asian Zonal Circulation
816 Index, Indian Ocean Dipole Mode Index and East Asian Summer Monsoon Index.
817 **Figure 10.** Similar to Figure 8 but for East Asian monsoon-dominated TP basins. It
818 should be noted that the GlobSnow data are not available for some basins. The double
819 red stars showed that the trend was statistically significant at the 0.05 level.
820 **Figure 11.** Similar to Figure 8 but for Indian monsoon-dominated TP basins. It should
821 be noted that the GlobSnow data are not available for some basins. The double red
822 stars showed that the trend was statistically significant at the 0.05 level.

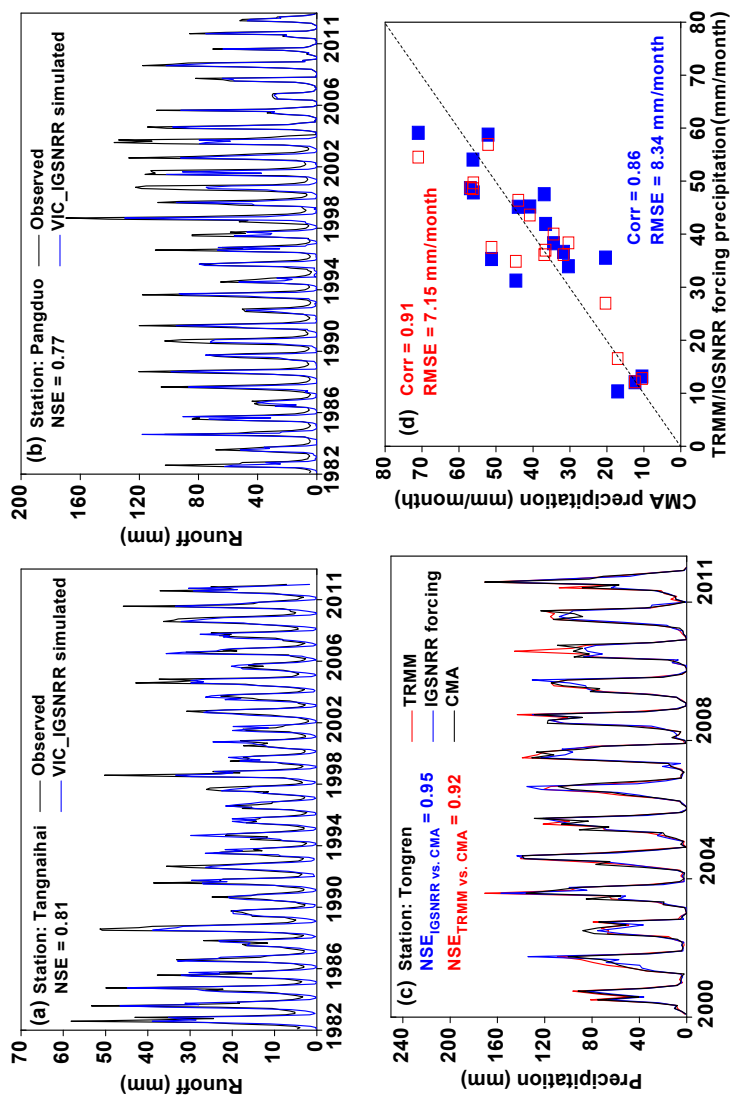


823 **Figure 1.** Map of river basins and hydrological gauging stations (green dots) over the Tibetan Plateau (TP) used in this study. The grey shading shows the
824 topography of TP in meters above the sea level and the blue shading exhibits the glaciers distribution in TP extracted from the Second Glacier Inventory Dataset of
825 China.





828 **Figure 2.** Comparison of VIC_IGSNRR simulated and observed monthly runoff for Tangnaihui and Panduo stations (a and b) as well as (c) basin-averaged
 829 monthly TRMM, CMA gridded and IGSNRR forcing precipitations for the smallest basin (Tongren station) over the period 1982-2011. (d) shows the comparison of
 830 TRMM (blue) and IGSNRR forcing (red) precipitations against CMA gridded precipitation for 18 river basins over TP during the period 2000-2011.

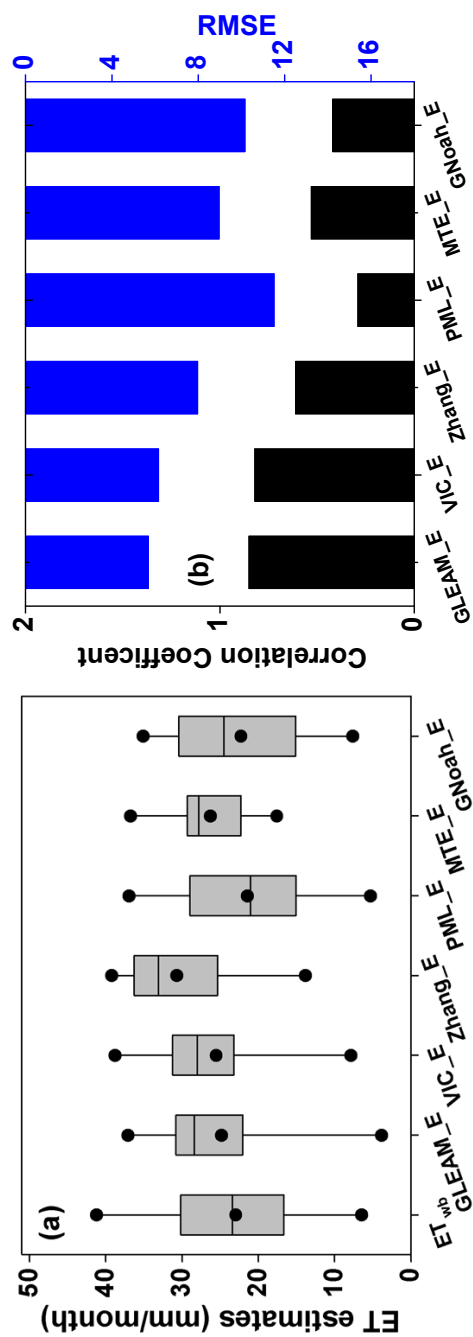


831

832
 833

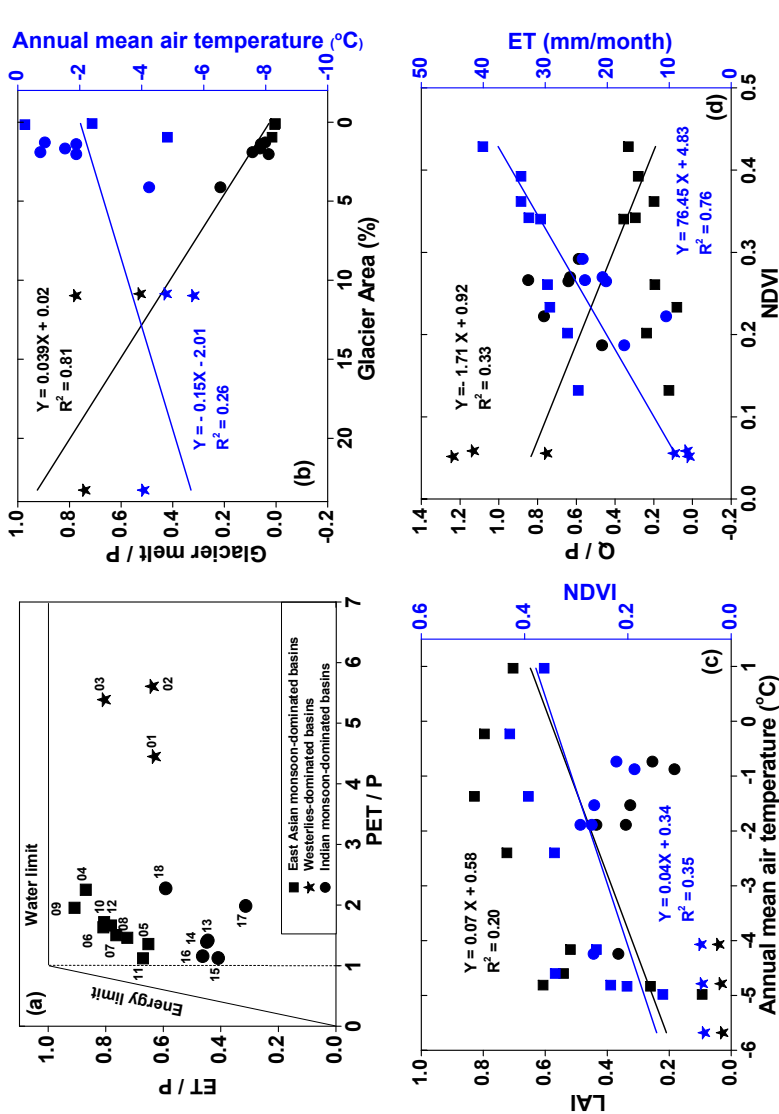


834 **Figure 3.** Comparison of different ET products against the calculated ET through the water balance (ET_{wb}) for 18 river basins over the Tibetan Plateau. The
 835 boxplot of annual estimates of different ET products for 18 TP basins are shown in (a) while the correlation coefficients and root-mean-square-errors (RMSEs,
 836 mm/month) for each ET product relatively to ET_{wb} are exhibited in (b).





839 **Figure 4.** General water and energy status (a. the perspective of Budyko framework) and their relationships with glacier (b) and vegetation (c and d) for eighteen
 840 TP river basins (1983-2006). The ET used in this figure is calculated from the bias-corrected water balance method.

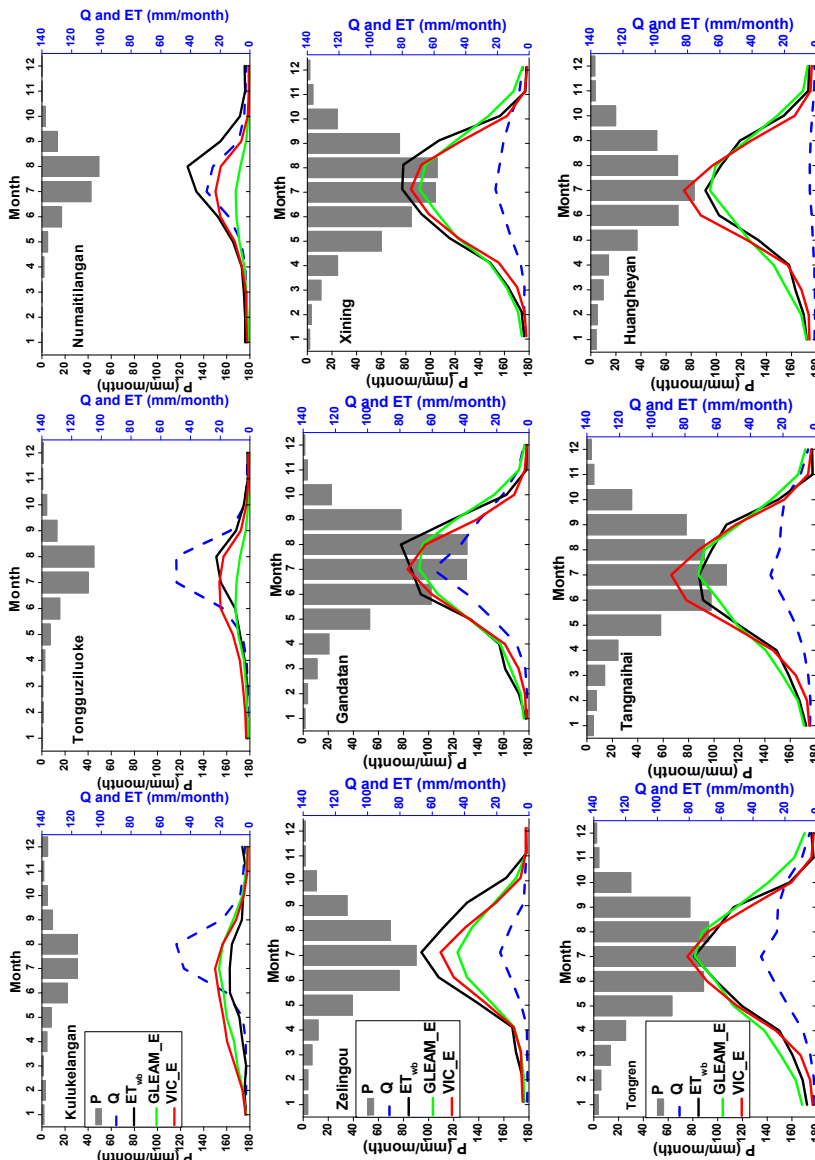


841

842



843 **Figure 5.** Seasonal cycles (1982-2011) of water budget components in westerlies-dominated (column 1), East Asian monsoon-dominated (columns 2-4) and Indian
 844 monsoon-dominated (columns 5-6) TP basins.



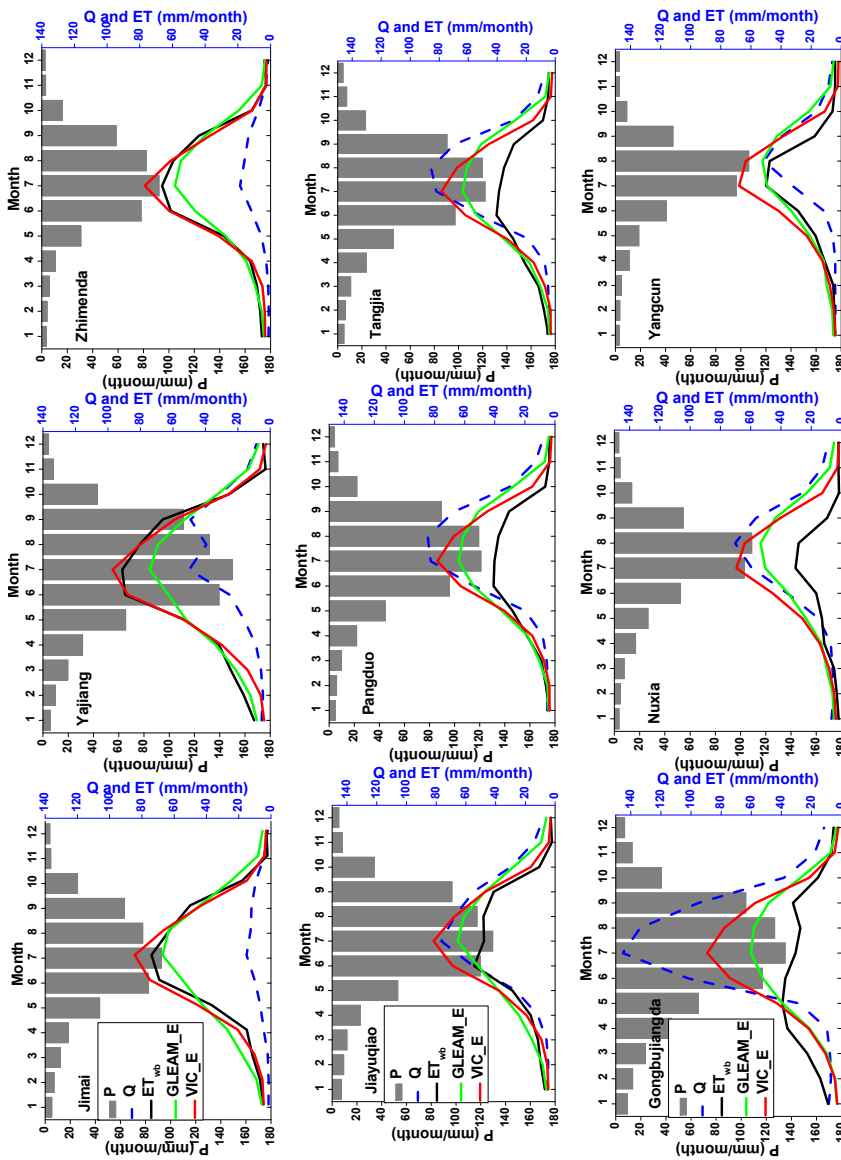
845

846

847



Figure 5: (continued)



848

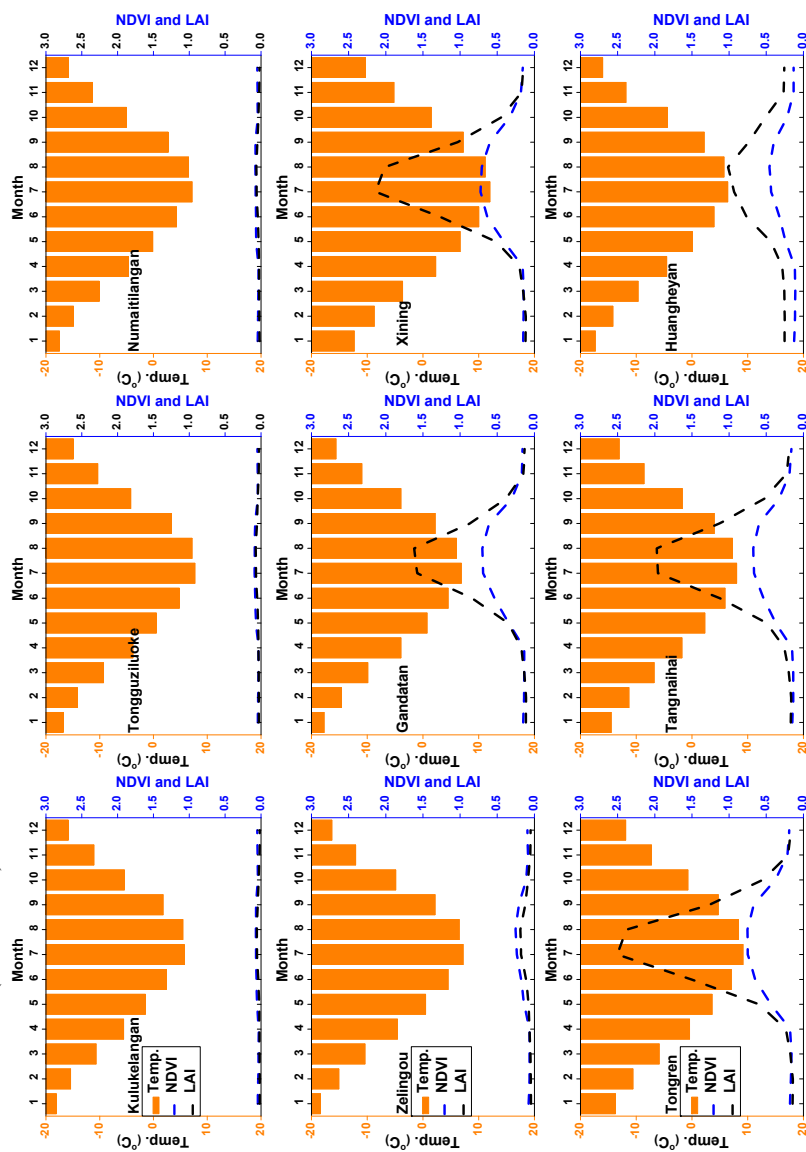
849

850

851



852 **Figure 6.** Seasonal cycles (1982-2011) of air temperature and vegetation parameters in westerlies-dominated (column 1), East Asian monsoon-dominated (columns
 853 2-4) and Indian monsoon-dominated (columns 5-6) TP basins.



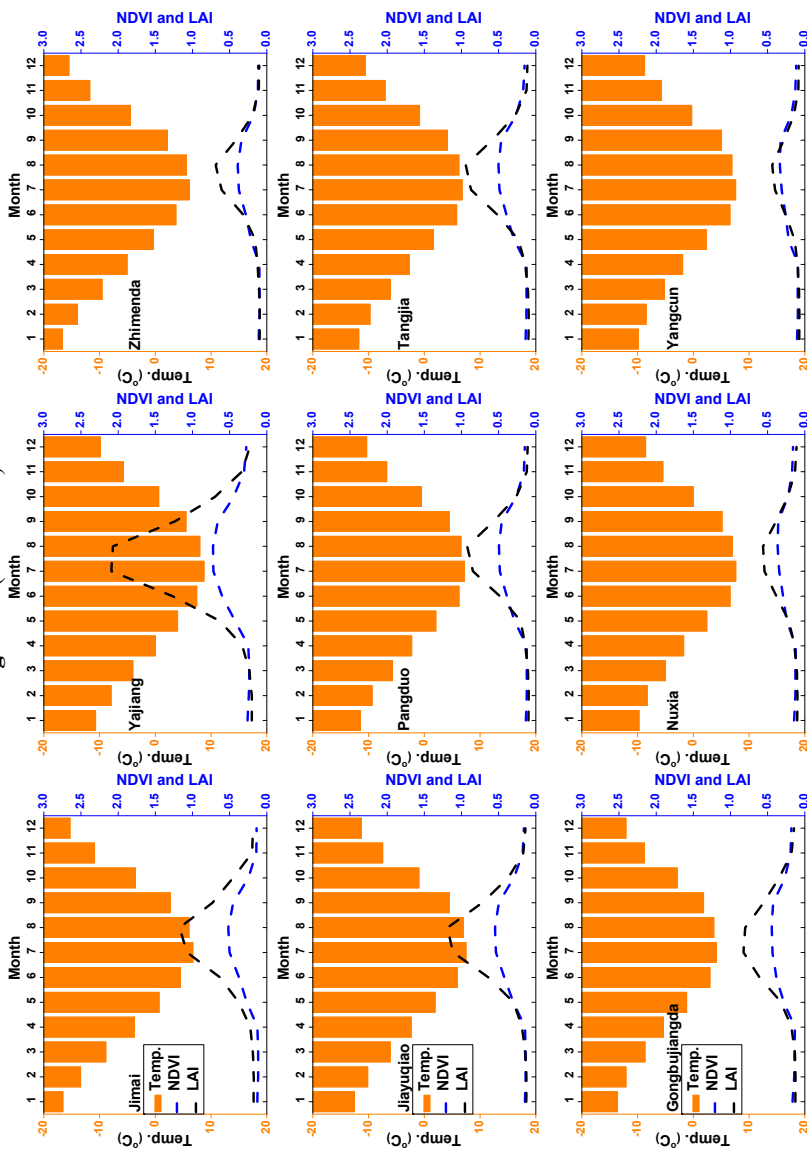
854

855

856



Figure 6: (continued)



857

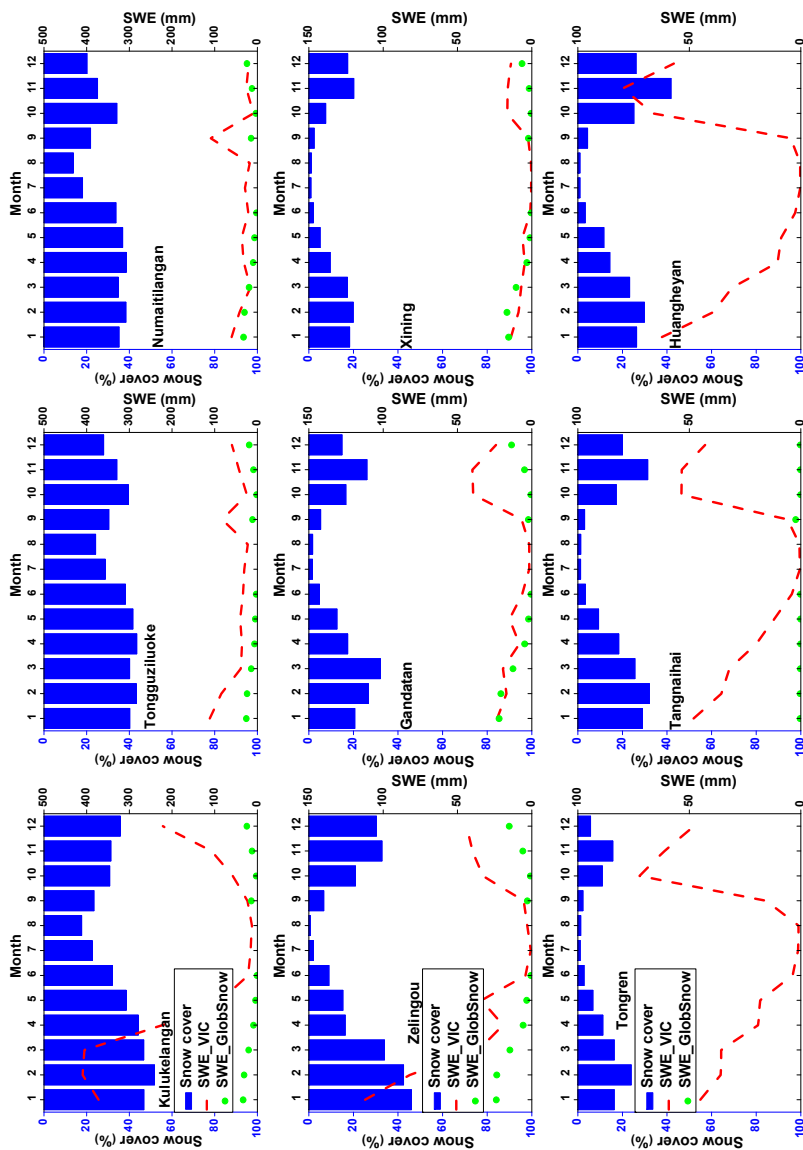
858

859

860
861



862 **Figure 7.** Seasonal cycles (1982-2011) of snow cover and snow water equivalent (SWE) in westerlies-dominated (column 1), East Asian monsoon-dominated
863 (columns 2-4) and Indian monsoon-dominated (columns 5-6) TP basins. The snow cover was extracted from cloud free snow composite product during the period
864 2005-2013. It should also be noted that the GlobSnow data are not available for some basins.
865

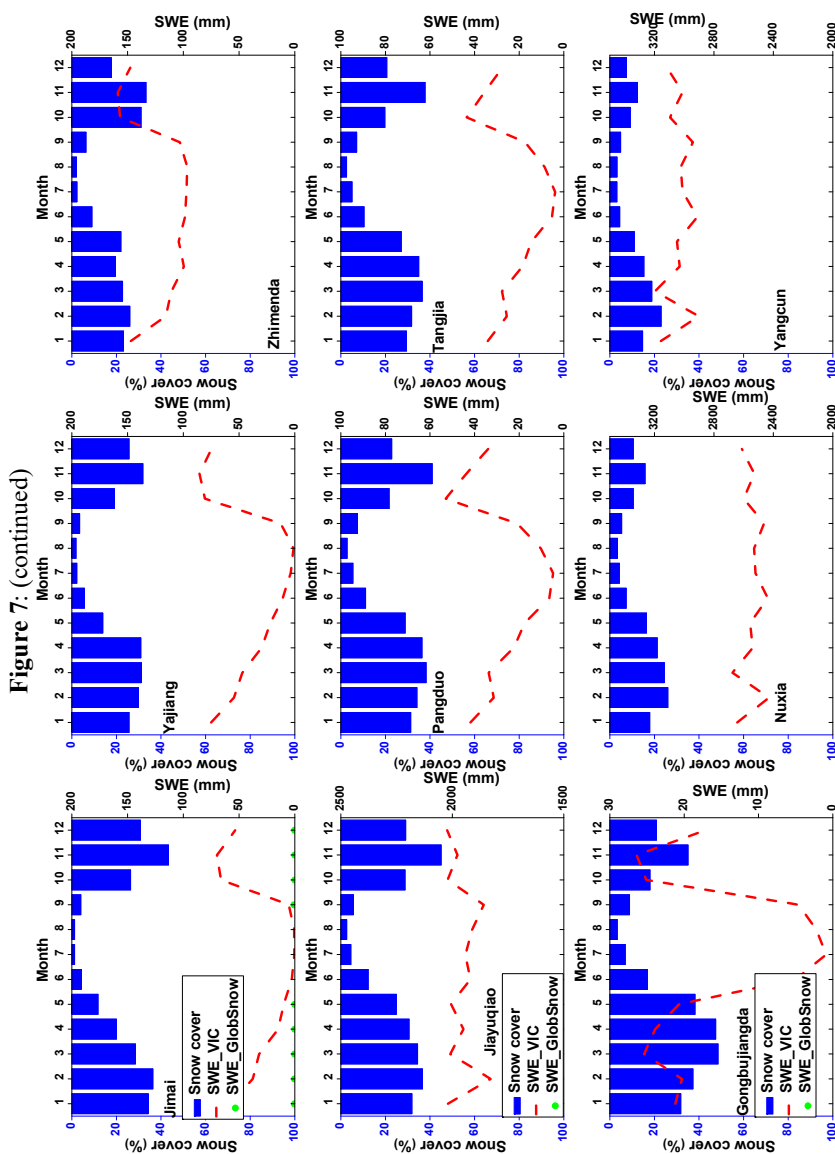


866

867

868

869
870

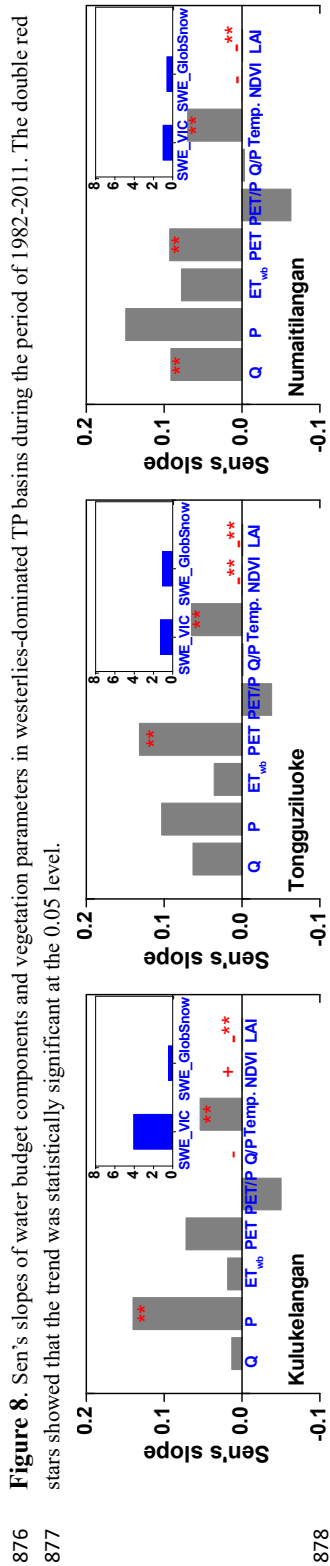


871

872

873

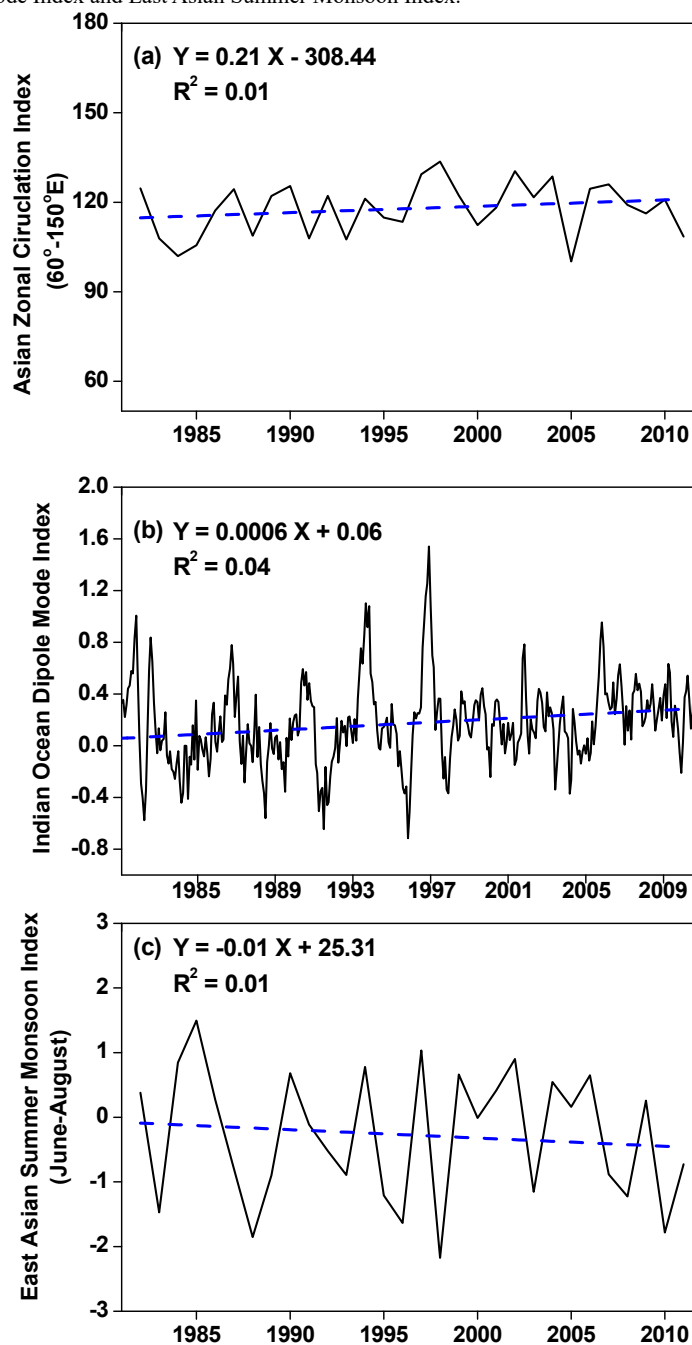
874
875



878
 879



880 **Figure 9.** Linear trends of westerly, Indian monsoon and East Asian summer monsoon during the
881 period 1982-2011 revealed prospectively by the Asian Zonal Circulation Index, Indian Ocean
882 Dipole Mode Index and East Asian Summer Monsoon Index.



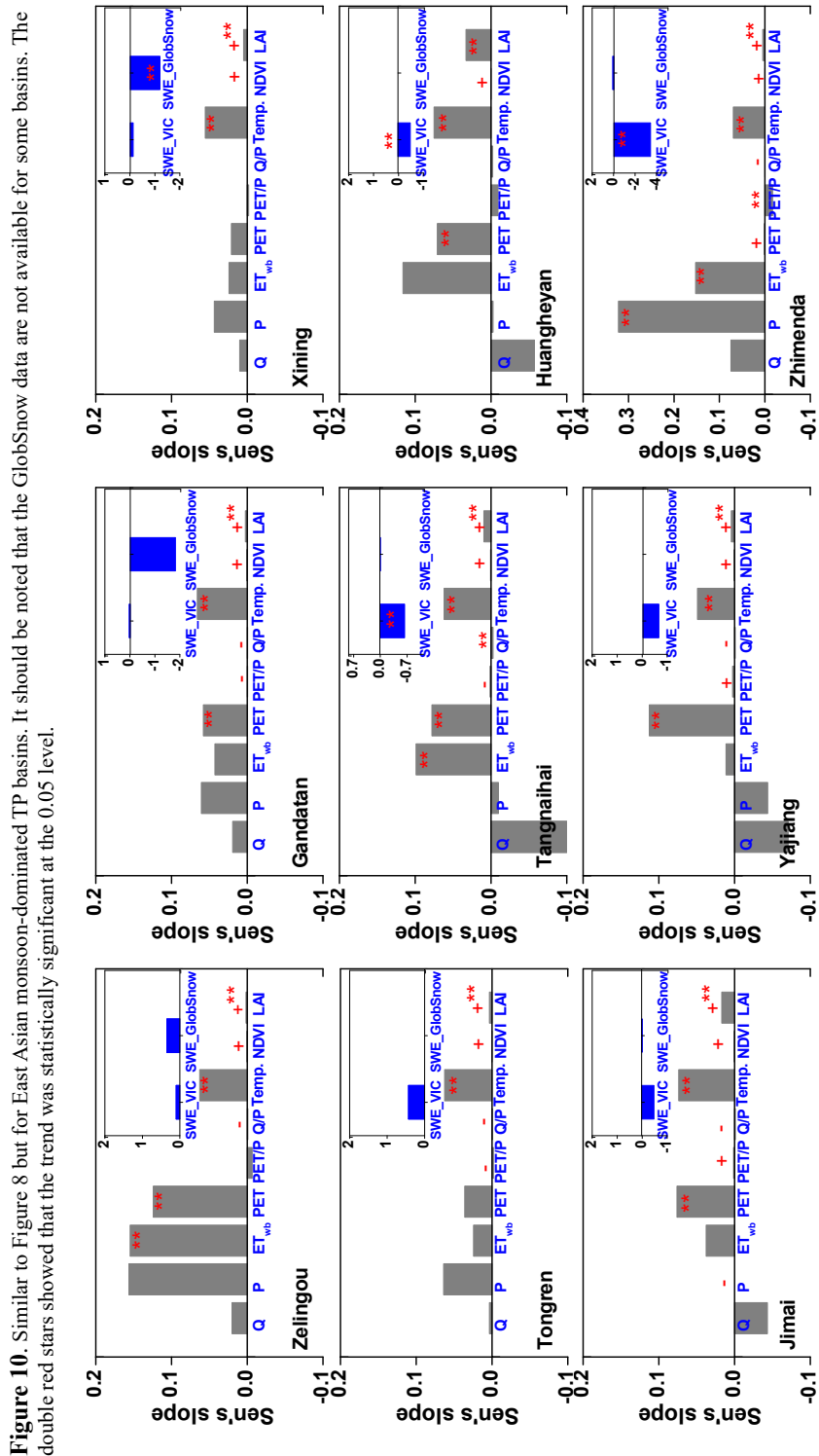
883

884

885

886

887



888 **Figure 10.** Similar to Figure 8 but for East Asian monsoon-dominated TP basins. It should be noted that the GlobSnow data are not available for some basins. The
 889 double red stars showed that the trend was statistically significant at the 0.05 level.
 890

888
 889
 890

891

892

893
 894
 895

